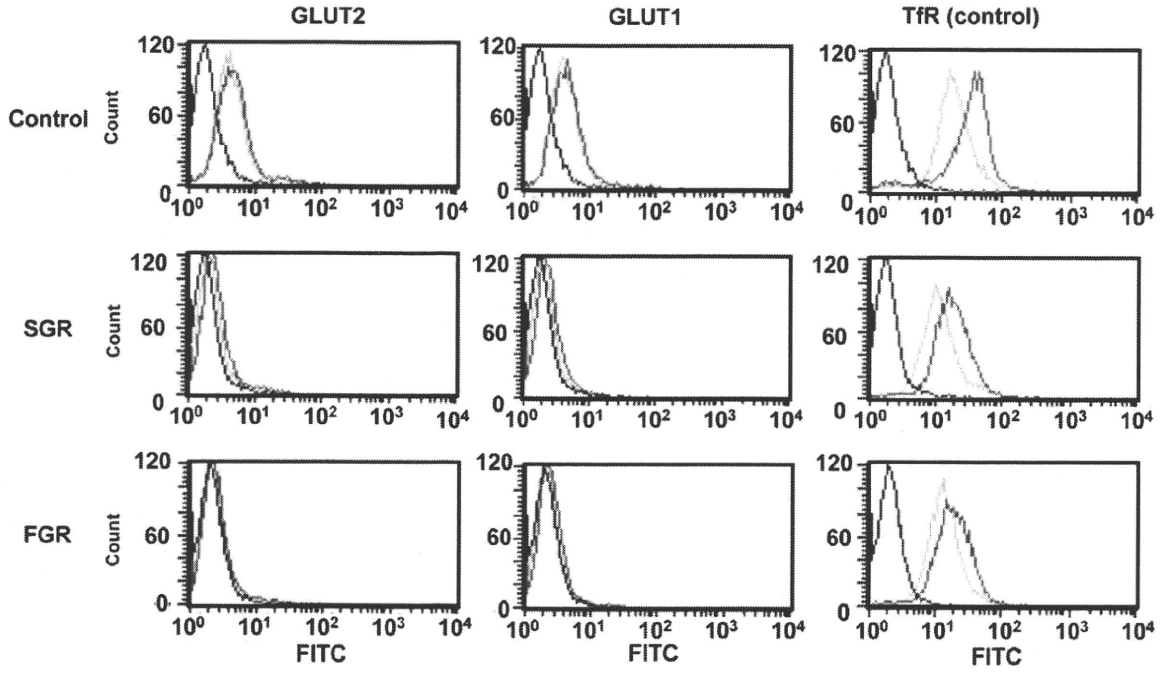

Fig. 5. Effects of lactacystin treatment on cell surface expression of GLUT2, GLUT1 and transferrin receptor (TfR). Cells were treated with lactacystin (10 μM) overnight to inhibit proteasomal degradation, and analyzed by flow cytometry. Cells treated with lactacystin are shown in red line and those left untreated in blue line. The negative controls stained with FITC-conjugated antibody alone are shown in black line.

of GLUT1 and GLUT2 expression is primarily involved in the decreased glucose uptake in SGR, FGR and HCV-infected cells.

3.8. Decreased GLUT2 expression in hepatocytes obtained from HCV-infected patients

GLUT2 is the principal glucose transporter expressed in hepatocytes *in vivo*. As shown in Fig. 7B, practically all hepatocytes obtained from patients without HCV infection showed positive staining for GLUT2, which was most evidently observed near the plasma membrane. On the other hand, hepatocytes obtained from HCV-infected patients showed markedly reduced GLUT2 staining in most, if not the entire, areas of the section, compared with the uninfected control (Fig. 7D). This heterogeneous staining pattern might reflect concomitant presence of areas comprising either virus-infected or uninfected hepatocytes in a tissue sample. Whereas all the sections obtained from 8 patients without HCV infection showed evenly positive staining for GLUT2, sections from 8 (89%) of 9 HCV-infected patients showed moderately to markedly reduced GLUT2 staining (Table 2). Reduced GLUT2 staining was observed also with hepatocytes in the liver tissues obtained from HBV-infected patients. However, the areas of reduced GLUT2 staining appeared to be more restricted in sections obtained from HBV-infected patients than in those from HCV-infected ones.

4. Discussion

HCV infection is known as an initiation and precipitating factor of type 2 diabetes [7–10,26,27]. Progression of liver fibrosis induced by persistent viral infection may induce diabetes [28]. Furthermore, it has been reported that the prevalence of diabetes is higher among patients with HCV-associated liver cirrhosis than in those with HBV-associated cirrhosis [7]. It is likely, therefore, that HCV infection itself is a risk factor of diabetes. Previous reports suggest that HCV infection directly causes insulin resistance that would cause the progression of diabetes [29–31]. However, the underlying mechanism(s) is not yet completely elucidated. In this study, we analyzed the effect of HCV infection on cellular glucose uptake and expression of glucose transporters.

We observed that glucose uptake was suppressed in cells harboring HCV RNA replicons (SGR and FGR) and those infected with HCV than in the control cells (Fig. 3). It has been reported that glucose disposal *in vivo* occurs through both insulin-dependent and insulin-independent mechanism [32]. We observed that treatment of SGR, FGR and the control Huh-7.5 cells with insulin (10^{-4} M to 10^{-9} M) increased glucose uptake by only about 50% from their basal levels (data not shown). Nevertheless, decreased glucose uptake by HCV-infected hepatocytes is a potential cause of hyperglycemia as the liver is a big organ accounting for 2% of the total body weight.

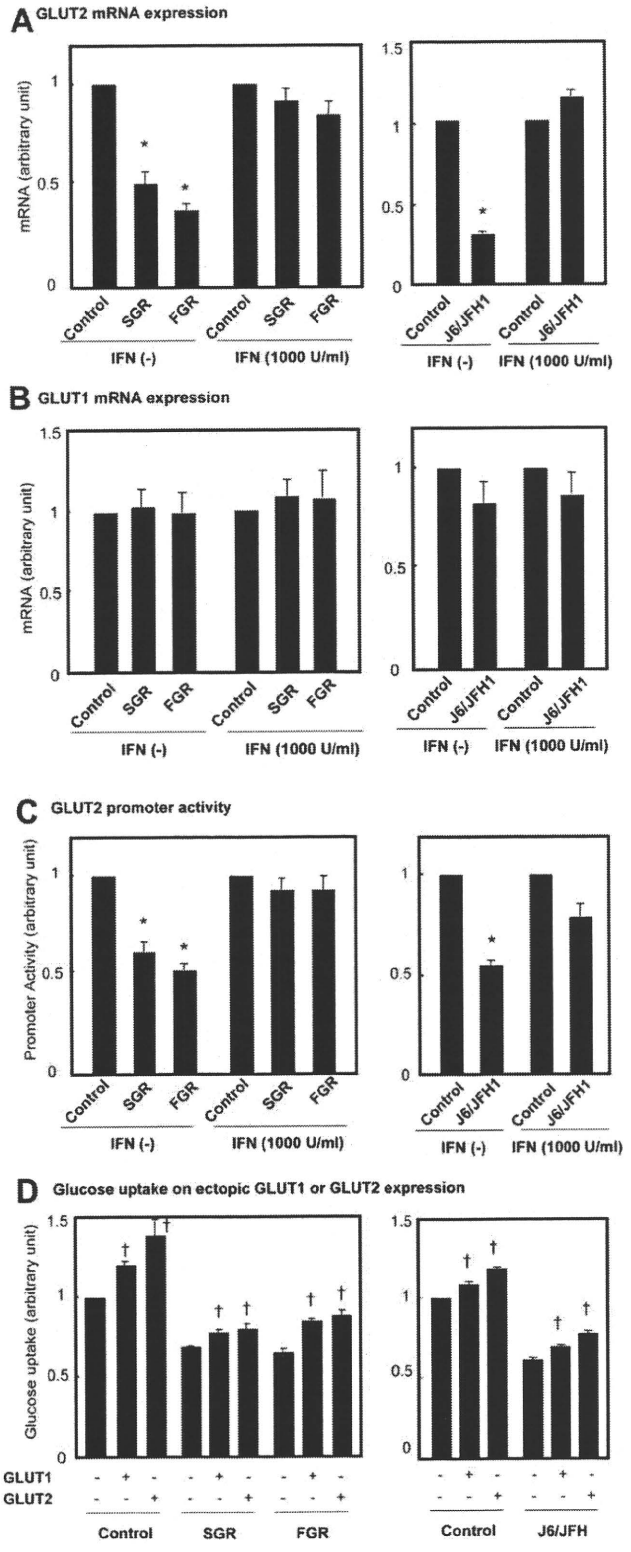

Fig. 6. Differential suppression of GLUT2 and GLUT1 mRNAs by HCV replication. (A and B) Quantitative RT-PCR analysis of mRNA for GLUT2 (A) and GLUT1 (B). mRNA expression levels of GLUT2 and GLUT1 in SGR, FGR and HCV-infected cells were determined and normalized with β-glucuronidase mRNA levels. In parallel, cells were treated with IFN (1000 IU/ml) for 10 days to eliminate HCV replication before being subjected to quantitative RT-PCR analysis. Data represent mean ± SEM of three independent experiments. $^{*}P < 0.01$, compared with the control. (C) GLUT2 promoter activities in SGR and FGR, HCV-infected cells were analyzed using luciferase reporter assay. In parallel, cells were treated with IFN (1000 IU/ml) for 10 days to eliminate HCV replication before being subjected to luciferase reporter assay. Data represent mean ± SEM of five independent experiments. $^{*}P < 0.01$, compared with the control. (D) Glucose uptake in cells ectopically expressing GLUT1 or GLUT2. Data represent mean ± SEM of two independent experiments. $^{\dagger}P < 0.01$, compared with mock transfected control.

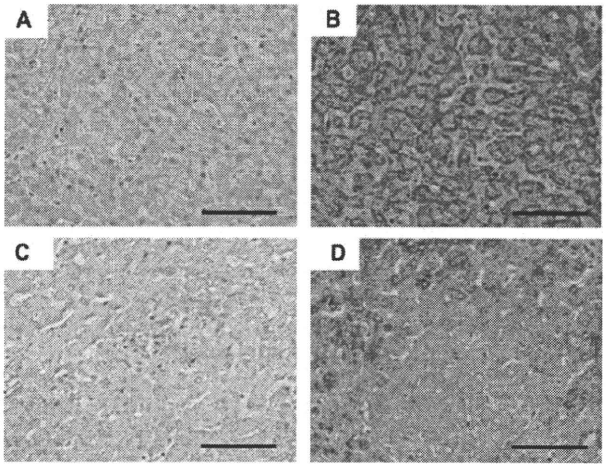

Fig. 7. Down-regulation of GLUT2 expression in HCV-infected human liver tissues *in vivo*. Normal human adult liver tissues (A and B) and HCV-infected, non-cancerous liver tissues (C and D) were fixed with formalin, sectioned and stained with normal rabbit IgG (A and C) or polyclonal anti-GLUT2 antibody (B and D). Scale bar = 100 μm.

Any proliferating cell requires energy sources, including glucose, and GLUTs play an important role in glucose uptake into the cell. In the liver, GLUT2 is the predominant glucose transporter, which regulates glucose metabolism by mediating a bidirectional transport, both entry and exit, of glucose into and from hepatocytes [13]. GLUT1, on the other hand, is known to be expressed in malignant cells including hepatocellular carcinoma [12,13] and a wide variety of cultured cells. In the present study we found that cell surface expression of GLUT2 and GLUT1 was markedly suppressed in SGR, FGR and HCV-infected cells compared to the control (Fig. 4A and B).

Table 2
Reduction of GLUT2 expression in hepatocytes of HCV-infected and HBV-infected human liver tissues.

Liver tissues	Sample No.	Reduction of GLUT2 expression
Uninfected	1	– *
	2	–
	3	–
	4	–
	5	–
	6	–
	7	–
	8	–
HCV-infected	9	1+ (Focal)[a]
	10	1+ (Focal)
	11	3+ (Diffuse)
	12	3+ (Diffuse)
	13	3+ (Diffuse)
	14	3+ (Focal)
	15	–
	16	2+ (Focal)
	17	3+ (Diffuse)
HBV-infected	18	–
	19	3+ (Diffuse)
	20	1+ (Focal)
	21	–
	22	2+ (Focal)
	23	1+ (Focal)
	24	2+ (Focal)

* -, no reduction; 1+, weak reduction; 2+, moderate reduction; 3+, strong reduction.

[a] Parentheses indicate either focal or diffuse appearance of the areas with reduced GLUT2 expression in each liver tissue sample.

GLUT2 expression is regulated at the transcriptional level, at least partly, by glucose [33]. It has been reported that hyperglycemia increases the GLUT2 mRNA and protein expression in an *in vivo* study [34]. Our present study demonstrated that GLUT2 mRNA expression was significantly suppressed in SGR, FGR and HCV-infected cells compared to the control (Fig. 6A). Consistent with this result, GLUT2 promoter activities, as measured by luciferase reporter assay, were suppressed in SGR, FGR and HCV-infected cells (Fig. 6C). In this connection, it was reported that GLUT2 promoter activities were up-regulated by sterol response element-binding protein (SREBP)-1c [35,36]. We confirmed in our study that GLUT2 promoter activities were up-regulated by over-expression of human SREBP-1c, and that the SREBP-1c-mediated GLUT2 promoter activities were suppressed significantly in SGR, FGR and HCV-infected cells (data not shown).

Unlike GLUT2 mRNA, GLUT1 mRNA was not suppressed by HCV RNA replication or HCV infection (Fig. 6B). Nevertheless, cell surface expression of GLUT1 was markedly down-regulated in SGR and FGR cells (Fig. 4A). As GLUT1 surface expression was not restored by treatment with lactacystin, a potent proteasome inhibitor (Fig. 5), it was unlikely that HCV-mediated suppression of GLUT1 surface expression was mediated through increased degradation by the ubiquitin-proteasome system. We assume that intracellular trafficking of GLUT1 (and possibly GLUT2 as well) is impaired by HCV RNA replication although we could not precisely prove it due mainly to the lack of an appropriate antibody that enables us to monitor GLUT1 trafficking. Further study is needed to elucidate the issue.

By means of immunohistochemical analysis, we confirmed that GLUT2 was strongly expressed in hepatocytes of the liver tissues obtained from all of 8 individuals without HCV infection (Fig. 7B and Table 2). More importantly, we demonstrated that GLUT2 expression was significantly down-regulated in hepatocytes obtained from 8 of 9 HCV-infected patients (Fig. 7D and Table 2). Interestingly, the areas where GLUT2 down-regulation was observed appeared to be scattered across the liver tissue sections. This may reflect the general observation that a group of hepatocytes in limited areas of the hepatic lobules, but not all the hepatocytes, are infected with HCV *in vivo*. By means of real-time quantitative PCR analysis, we found a tendency that levels of GLUT2 mRNA expression in liver tissues obtained from HCV-infected patients were lower than that obtained from uninfected controls although the dif-

ference was not statistically significant (data not shown). As stated above, not all the hepatocytes in the liver were infected with HCV and, therefore, the possible reduction of GLUT2 mRNA expression in HCV-infected hepatocytes might have been masked by the normal levels of expression in uninfected hepatocytes concomitantly present in the same tissue samples.

It should also be noted that GLUT2 staining was also reduced in hepatocytes obtained from HBV-infected patients, though to a lesser extent than that from HCV-infected ones (Table 2). We assume that inflammatory responses in the liver may trigger some intracellular event that leads to decreased GLUT2 expression in hepatocytes *in vivo*.

In conclusion, we have demonstrated for the first time that HCV replication inhibits cellular glucose uptake through down-regulation of cell surface expression of GLUT2 and possibly GLUT1. It is conceivable that the decreased glucose uptake by hepatocytes causes impaired glucose metabolism, leading eventually to the initiation and progression of diabetes mellitus during a prolonged period of HCV persistence.

Acknowledgements

The authors are grateful to Dr. C.M. Rice (The Rockefeller University, New York, NY, USA) for providing pFL-J6/JFH1 and Huh7.5 cells. Thanks are also due to Dr. R. Bartenschlager (University of Heidelberg, Heidelberg, Germany) for providing an HCV subgenomic RNA replicon (pFK5B/2884Gly) and Dr. R. Sato (The University of Tokyo, Tokyo, Japan) for providing a human SREBP-1c expression plasmid (pME-hSREBP-1c). This study was supported in part by grants-in-aid for Scientific Research from the Ministry of Education, Culture, Sports, Science and Technology (MEXT) and the Ministry of Health, Labour and Welfare, Japan. This study was also carried out as part of the Program of Founding Research Centers for Emerging and Reemerging Infectious Diseases, MEXT, Japan, and the Global Center of Excellence (COE) Program at Kobe University Graduate School of Medicine.

Appendix A. Supplementary data

Supplementary data associated with this article can be found, in the online version, at doi:10.1016/j.jhep.2008.12.029.

References

[1] Simmonds P, Bukh J, Combet C, Deléage G, Enomoto N, Feinstone S, et al. Consensus proposals for a unified system of nomenclature of hepatitis C virus genotypes. Hepatology 2005;42:962–973.

[2] Lu L, Li C, Fu Y, Thaikruea L, Thongswat S, Maneekarn N, et al. Complete genomes for hepatitis C virus subtypes 6f, 6i, 6j and 6m: viral genetic diversity among Thai blood donors and infected spouses. J Gen Virol 2007;88:1505–1518.

[3] Lindenbach BD, Rice CM. Unravelling hepatitis C virus replication from genome to function. Nature 2005;436:933–938.

[4] Appel N, Schaller T, Penin F, Bartenschlager R. From structure to function: new insights into hepatitis C virus RNA replication. J Biol Chem 2006;281:9833–9836.

[5] Shepard CW, Finelli L, Alter MJ. Global epidemiology of hepatitis C virus infection. Lancet Infect Dis 2005;5:558–567.

[6] Galossi A, Guarisco R, Bellis L, Puoti C. Extrahepatic manifestations of chronic HCV infection. J Gastrointestin Liver Dis 2007;16:65–73.

[7] Caronia S, Taylor K, Pagliaro L, Carr C, Palazzo U, Petrik J, et al. Further evidence for an association between non-insulin-dependent diabetes mellitus and chronic hepatitis C virus infection. Hepatology 1999;30:1059–1063.

[8] Mason AL, Lau JY, Hoang N, Qian K, Alexander GJ, Xu L, et al. Association of diabetes mellitus and chronic hepatitis C virus infection. Hepatology 1999;29:328–333.

[9] Mehta S, Levey JM, Bonkovsky HL. Extrahepatic manifestations of infection with hepatitis C virus. Clin Liver Dis 2001;5:979–1008.

[10] Mehta SH, Brancati FL, Sulkowski MS, Strathdee SA, Szklo M, Thomas DL. Prevalence of type 2 diabetes mellitus among persons with hepatitis C virus infection in the United States. Ann Intern Med 2000;133:592–599.

[11] Wu X, Freeze HH. GLUT14, a duplicon of GLUT3, is specifically expressed in testis as alternative spice forms. Genomics 2002;80:553–557.

[12] Macheda ML, Rogers S, Best JD. Molecular and cellular regulation of glucose transporter (GLUT) proteins in cancer. J Cell Physiol 2005;202:654–662.

[13] Godoy A, Ulloa V, Rodriguez F, Reinicke K, Yanez AJ, Garcia Mde L, et al. Differential subcellular distribution of glucose transporters GLUT1-6 and GLUT9 in human cancer: ultrastructural localization of GLUT1 and GLUT5 in breast tumor tissues. J Cell Physiol 2006;207:614–627.

[14] Ban N, Yamada Y, Someya Y, Miyawaki K, Ihara Y, Hosokawa M, et al. Hepatocyte nuclear factor-1α recruits the transcriptional co-activator p300 on the GLUT2 gene promoter. Diabetes 2002;51:1409–1418.

[15] Blight KJ, McKeating JA, Rice CM. Highly permissive cell lines for subgenomic and genomic hepatitis C virus RNA replication. J Virol 2002;76:13001–13014.

[16] Hidajat R, Nagano-Fujii M, Deng L, Tanaka M, Takigawa Y, Kitazawa S, et al. Hepatitis C virus NS3 protein interacts with ELKS-δ and ELKS-α, members of a novel protein family involved in intracellular transport and secretory pathways. J Gen Virol 2005;86:2197–2208.

[17] Nomura-Takigawa Y, Nagano-Fujii M, Deng L, Kitazawa S, Ishido S, Sada K, et al. Non-structural protein 4A of Hepatitis C virus accumulates on mitochondria and renders the cells prone to undergoing mitochondria-mediated apoptosis. J Gen Virol 2006;87:1935–1945.

[18] Inubushi S, Nagano-Fujii M, Kitayama K, Tanaka M, An C, Yokozaki H, et al. Hepatitis C virus NS5A protein interacts with and negatively regulates the non-receptor protein–tyrosine kinase Syk. J Gen Virol 2008;89:1231–1242.

[19] Ikeda M, Abe K, Dansako H, Nakamura T, Naka K, Kato N. Efficient replication of a full-length hepatitis C virus genome, strain O, in cell culture, and development of a luciferase reporter system. Biochem Biophys Res Commun 2005;329:1350–1359.

[20] Deng L, Nagano-Fujii M, Tanaka M, Nomura-Takigawa Y, Ikeda M, Kato N, et al. NS3 protein of Hepatitis C virus associates with the tumour suppressor p53 and inhibits its

function in an NS3 sequence-dependent manner. J Gen Virol 2006;87:1703–1713.
[21] Lindenbach BD, Evans MJ, Syder AJ, Wolk B, Tellinghuisen TL, Liu CC, et al. Complete replication of hepatitis C virus in cell culture. Science 2005;309:623–626.
[22] Deng L, Adachi T, Kitayama K, Bungyoku Y, Kitazawa S, Ishido S, et al. Hepatitis C virus infection induces apoptosis through a Bax-triggered, mitochondrion-mediated, caspase 3-dependent pathway. J Virol 2008;82:10375–10385.
[23] Kanda H, Tamori Y, Shinoda H, Yoshikawa M, Sakaue M, Udagawa J, et al. Adipocytes from Munc18c-null mice show increased sensitivity to insulin-stimulated GLUT4 externalization. J Clin Invest 2005;115:291–301.
[24] Niwa H, Yamamura K, Miyazaki J. Efficient selection for high-expression transfectants with a novel eukaryotic vector. Gene 1991;108:193–199.
[25] Lehner PJ, Hoer S, Dodd R, Duncan LM. Downregulation of cell surface receptors by the K3 family of viral and cellular ubiquitin E3 ligase. Immunol Rev 2005;207:112–125.
[26] Mehta SH, Brancati FL, Strathdee SA, Pankow JS, Netski D, Coresh J, et al. Hepatitis C virus infection and incident type 2 diabetes. Hepatology 2003;38:50–56.
[27] Wang CS, Wang ST, Yao WJ, Chang TT, Chou P. Hepatitis C virus infection and the development of type 2 diabetes in a community-based longitudinal study. Am J Epidemiol 2007;166:196–203.
[28] Hui JM, Sud A, Farrell GC, Bandara P, Byth K, Kench JG, et al. Insulin resistance is associated with chronic hepatitis C virus infection and fibrosis progression. Gastroenterology 2003;125:1695–1704.
[29] Kawaguchi T, Yoshida T, Harada M, Hisamoto T, Nagao Y, Ide T, et al. Hepatitis C virus down-regulates insulin receptor substrates 1 and 2 through up-regulation of suppressor of cytokine signaling 3. Am J Pathol 2004;165:1499–1508.
[30] Miyamoto H, Moriishi K, Moriya K, Murata S, Tanaka K, Suzuki T, et al. Involvement of the PA28γ-dependent pathway in insulin resistance induced by hepatitis C virus core protein. J Virol 2007;81:1727–1735.
[31] Ader M, Ni TC, Bergman RN. Glucose effectiveness assessed under dynamic and steady state conditions. Comparability of uptake versus production components. J Clin Invest 1997;99:1187–1199.
[32] Banerjee S, Saito K, Ait-Goughoulte M, Meyer K, Ray RB, Ray R. Hepatitis C virus core protein upregulates serine phosphorylation of IRS-1 and impairs downstream Akt/PKB signaling pathway for insulin resistance. J Virol 2008;82:2606–2612.
[33] Im SS, Kim SY, Kim HI, Ahn YH. Transcriptional regulation of glucose sensors in pancreatic beta cells and liver. Curr Diabetes Rev 2006;2:11–18.
[34] Adachi T, Yasuda K, Okamoto Y, Shihara N, Oku A, Ueta K, et al. T-1095, a renal Na^+-glucose transporter inhibitor, improves hyperglycemia in streptozotocin-induced diabetic rats. Metabolism 2000;49:990–995.
[35] Im SS, Kang SY, Kim SY, Kim HI, Kim JW, Kim KS, et al. Glucose-stimulated upregulation of GLUT2 gene is mediated by sterol response element-binding protein-1c in the hepatocytes. Diabetes 2005;54:1684–1691.
[36] Kanayama T, Arito M, So K, Hachimura S, Inoue J, Sato R. Interaction between sterol regulatory element-binding proteins and liver receptor homolog-1 reciprocally suppresses their transcriptional activities. J Biol Chem 2007;282:10290–10298.

Journal of General Virology (2009), **90**, 1681–1691 DOI 10.1099/vir.0.010983-0

Efficient production of infectious hepatitis C virus with adaptive mutations in cultured hepatoma cells

Yasuaki Bungyoku, Ikuo Shoji, Tatsuhiko Makine, Tetsuya Adachi, Kazumi Hayashida, Motoko Nagano-Fujii, Yoshi-Hiro Ide, Lin Deng and Hak Hotta

Division of Microbiology, Kobe University Graduate School of Medicine, 7-5-1 Kusunoki-cho, Chuo-ku, Kobe, Hyogo 650-0017, Japan

Correspondence
Hak Hotta
hotta@med.kobe-u.ac.jp

Received 11 February 2009
Accepted 5 March 2009

Robust production of infectious hepatitis C virus (HCV) in cell culture was realized by using the JFH1 strain and the homologous chimeric J6/JFH1 strain in Huh-7.5 cells, a highly HCV-permissive subclone of Huh-7 cells. In this study, we aimed to establish a more efficient HCV-production system and to gain some insight into the adaptation mechanisms of efficient HCV production. By serial passaging of J6/JFH1-infected Huh-7.5 cells, we obtained culture-adapted J6/JFH1 variants, designated P-27, P-38 and P-47. Sequence analyses revealed that the adaptive mutant viruses P-27, P-38 and P-47 possessed eight mutations [four in E2, two in NS2, one in NS5A and one in NS5B), 10 mutations [two additional mutations in the 5′-untranslated region (5′-UTR) and core] and 11 mutations (three additional mutations in 5′-UTR, core and NS5B), respectively. We introduced amino acid substitutions into the wild-type J6/JFH1 clone, generated recombinant viruses with adaptive mutations and analysed their infectivity and ability to produce infectious viruses. The viruses with the adaptive mutations exhibited higher expression of HCV proteins than did the wild type in Huh-7.5 cells. Moreover, we provide evidence suggesting that the mutation N534H in the E2 glycoprotein of the mutant viruses conferred an advantage at the entry level. We thus demonstrate that an efficient HCV-production system could be obtained by introducing adaptive mutations into the J6/JFH1 genome. The J6/JFH1-derived mutant viruses presented here would be a good tool for producing HCV particles with enhanced infectivity and for studying the molecular mechanism of HCV entry.

INTRODUCTION

Hepatitis C virus (HCV) is the main cause of chronic hepatitis, liver cirrhosis and hepatocellular carcinoma (Choo *et al.*, 1989; Kuo *et al.*, 1989; Saito *et al.*, 1990). As more than 170 million people worldwide are infected chronically with HCV (Poynard *et al.*, 2003) and because the current antiviral therapy, interferon and ribavirin, produces sustained virus clearance in <50 % of treated patients (Manns *et al.*, 2007), HCV infection is clearly a problem of major proportions. HCV is a single-stranded, positive-sense RNA virus that is classified in the genus *Hepacivirus* in the family *Flaviviridae*. The approximately 9.6 kb HCV genome encodes one large open reading frame (ORF) that is flanked at the 5′ and 3′ ends by untranslated regions (UTRs) (Choo *et al.*, 1991). The HCV polyprotein is processed into at least 10 proteins by viral proteases and cellular signalases (Grakoui *et al.*, 1993; Hijikata *et al.*, 1993a; McLauchlan *et al.*, 2002). The structural proteins core, E1 and E2 are located in the N terminus of the polyprotein, followed by p7 and the non-structural (NS) proteins NS2, NS3, NS4A, NS4B, NS5A and NS5B (Bartenschlager & Sparacio, 2007).

Study of the HCV life cycle and virus–host interaction has been hampered severely by the lack of a robust *in vitro* cell-culture system and small-animal models of HCV infection (Bartenschlager & Sparacio, 2007). The development of HCV replicon systems has made an important contribution to the study of HCV translation and RNA replication in the human hepatoma cell line Huh-7 (Blight *et al.*, 2000; Lohmann *et al.*, 1999). Sequence analyses of multiple HCV replicons have revealed that several adaptive mutations enhance RNA replication to varying degrees (Bartenschlager & Sparacio, 2007; Blight *et al.*, 2000; Lohmann *et al.*, 2001). Such adaptive mutations were primarily identified in a central portion of the NS5A protein. Although the extent to which these adaptive mutations enhance RNA replication was subsequently studied by using various transient replication assays, the molecular mechanism underlying replication enhancement still remains elusive (Bartenschlager & Sparacio, 2007). The HCV replicons containing adaptive mutations do not produce infectious virus particles in culture and are severely attenuated (Blight *et al.*, 2002; Pietschmann *et al.*, 2002). Using recombinant HCV envelope glycoproteins

and HCV pseudoparticles, several cell-surface molecules have been shown to interact with HCV during virus binding and entry, including the tetraspanin CD81 (Bartosch *et al.*, 2003; Pileri *et al.*, 1998), the scavenger receptor class B member I (SR-BI) (Bartosch *et al.*, 2003; Scarselli *et al.*, 2002) and the tight junction protein claudin-1 (CLDN1) (Evans *et al.*, 2007).

The major breakthrough was made by establishing an HCV-production system using HCV strain JFH1, a genotype 2a isolate, and Huh-7 cells (Wakita *et al.*, 2005). Two other groups reported a robust production of infectious virus using a homologous chimeric FL-J6/JFH1 strain (Lindenbach *et al.*, 2005) or using Huh-7.5.1 cells (Zhong *et al.*, 2005) derived from the cell line Huh-7.5, which has a defect in the RIG-I pathway (Sumpter *et al.*, 2005). Upon transfection of Huh-7 cells with the *in vitro*-transcribed HCV JFH1 genome or the chimera FL-J6/JFH1, infectious HCV particles were secreted in an envelope glycoprotein-dependent manner (Lindenbach *et al.*, 2005; Wakita *et al.*, 2005; Zhong *et al.*, 2005). Using HCV-production systems, adaptive or compensatory mutations that promote the production of infectious virus from wild-type JFH1 (Delgrange *et al.*, 2007; Kaul *et al.*, 2007; Russell *et al.*, 2008; Zhong *et al.*, 2006) or chimeric viruses (Gottwein *et al.*, 2007; Yi *et al.*, 2006, 2007) have been identified. However, the molecular mechanisms of adaptive mutations are poorly understood.

In this study, we aimed to establish an efficient HCV-production system and to gain more insight into the determinants of efficient virus production. By serial passaging of Huh-7.5 cells infected with the HCV J6/JFH1 strain, we identified adaptive mutations in the clones and analysed the mutations by examining the production of the recombinant mutant viruses.

METHODS

Cell culture. Huh-7.5 cells (Blight *et al.*, 2002), a highly HCV-permissive subclone of Huh-7 cells, were kindly provided by Dr C. M. Rice (Rockefeller University, New York, NY, USA). Cells were cultured in Dulbecco's modified Eagle's medium (DMEM; Wako) supplemented with 10 % fetal bovine serum (FBS; Biowest), 0.1 mM non-essential amino acids (Invitrogen), 100 IU penicillin ml^{-1} and 100 μg streptomycin ml^{-1} (Invitrogen). DMEM containing 10 % FBS was designated complete DMEM. Cells were grown at 37 °C in a CO_2 incubator.

Antibodies. The mouse monoclonal antibodies (mAbs) used in this study were anti-core (2H9) mAb (Wakita *et al.*, 2005) and anti-HCV NS3 mAb (Chemicon). Goat anti-actin polyclonal antibody (C-11) (Santa Cruz Biotech) was used. Horseradish peroxidase (HRP)-conjugated goat anti-mouse IgG (MBL) and HRP-conjugated donkey anti-goat IgG (Santa Cruz Biotech) were used as secondary antibodies.

Plasmids. Plasmid pFL-J6/JFH1 (Lindenbach *et al.*, 2005) containing the full-length chimeric HCV genome was used to generate infectious HCV. Amino acid substitutions were introduced by site-directed mutagenesis using a QuikChange site-directed mutagenesis kit (Stratagene). All PCR-amplified DNA fragments were verified extensively by using an ABI PRISM 3100-Avant Genetic Analyzer (Applied Biosystems). The primer sequences used in this study are available from the authors upon request.

HCV RNA transfection and virus production. The pFL-J6/JFH1 plasmid was linearized with *Xba*I and *in vitro*-transcribed by using the T7 RiboMAX Express large-scale RNA production system (Promega) following the manufacturer's instructions. The quality of synthesized RNA was examined by agarose gel electrophoresis. Cells were trypsinized and washed with serum-free DMEM. In total, 6×10^6 cells were suspended in 500 μl serum-free DMEM and mixed with 10 μg *in vitro*-transcribed RNA in a 4 mm cuvette (Bio-Rad). The synthesized RNA was introduced into Huh-7.5 cells by electroporation using a Bio-Rad Gene Pulser system with a single pulse at 270 V, 975 μF. The cells were then plated in 10 cm culture dishes containing complete DMEM.

Indirect immunofluorescence. Immunofluorescence staining was performed essentially as described previously (Takigawa *et al.*, 2004). Cells seeded on glass coverslips in a 24-well plate at a density of 4×10^4 cells per well were infected with HCV. Cells were cultured, washed with PBS and fixed with 3.7 % paraformaldehyde in PBS for 10 min at room temperature, followed by permeabilization in 0.1 % Triton X-100 in PBS for 10 min at room temperature. After being washed twice with PBS, cells were blocked with 5 % goat serum in PBS and then incubated with the serum of an HCV-infected patient with a high titre of anti-HCV antibodies. Fluorescein isothiocyanate-conjugated goat anti-human IgG (MBL) was used as a secondary antibody. The cells were washed with PBS, counterstained with Hoechst 33342 solution (Molecular Probes) at room temperature for 10 min, mounted on glass slides and examined under a fluorescence microscope (BX51; Olympus).

Virus titration. Culture supernatants were diluted serially 10-fold in complete DMEM and used to infect 2×10^5 naïve Huh-7.5 cells per well in 24-well plates. The inoculum was incubated with cells for 6 h at 37 °C and then supplemented with fresh complete DMEM. The level of HCV infection was determined 1 day post-infection by immunofluorescence using anti-HCV polyclonal antibody. The virus titre was expressed in focus-forming units (ml supernatant)$^{-1}$ (f.f.u. ml^{-1}), as determined by the mean number of HCV-positive foci detected at the highest dilutions according to a previously described method (Zhong *et al.*, 2005).

Immunoblotting. Immunoblotting was performed essentially as described previously (Muramatsu *et al.*, 1997). To detect the expression of HCV proteins, the immune complexes were visualized by an ECL Western blotting detection kit (GE Healthcare) following the manufacturer's instructions.

HCV RNA quantification. Total RNA was extracted by using RNAiso (TaKaRa) according to the manufacturer's instructions. One microgram of isolated RNA was reverse-transcribed by using a QuantiTect reverse transcription kit (Qiagen) with random primers. RT-qPCR analysis was performed as described previously (Zhong *et al.*, 2005). HCV RNA was monitored by using the PCR primers 5′-TCTGCGGAACCGGTGAGTA-3′ (sense) and 5′-TCAGGCAGTACCACAAGGC-3′ (antisense). HCV transcript levels were determined relative to a standard curve comprising serial dilutions of plasmid containing the HCV J6/JFH1 cDNA.

HCV RNA genome sequencing. HCV RNA was isolated from 140 μl viral supernatant by using a QIAamp Viral RNA Mini kit (Qiagen), and then used as a template to generate cDNA in a reverse-transcription reaction using SuperScript One-Step RT-PCR with Platinum *Taq* (Invitrogen) according to the manufacturer's instruc-

tions. PCR primers of between 20 and 26 bases, designed using the sequence of J6/JFH1, were used to amplify four fragments of HCV cDNA (nt 49–3517, 2582–5966, 5832–8038 and 7870–9286) to cover most of the HCV genome. In addition, the 5′-end sequence was amplified by using the 5′ RACE System for Rapid Amplification of cDNA Ends (Invitrogen) and the 3′-end sequence was amplified by using a 3′-Full RACE Core set (TaKaRa). The sequences of the amplified DNA were determined by using an ABI PRISM 3100-Avant Genetic Analyzer.

Quantification of HCV core protein. HCV core protein in the cells or cell-culture supernatants was quantified by using a highly sensitive enzyme immunoassay (Ortho HCV antigen ELISA kit; Ortho Clinical Diagnostics). To determine intracellular amounts of core, cell lysates were prepared as described by Schaller *et al.* (2007).

Blocking of virus attachment and entry with anti-CD81 antibody. Blocking of virus attachment and entry with anti-CD81 antibody was performed essentially as described previously (Wakita *et al.*, 2005). Huh-7.5 cells (6×10^4 cells per 24-well plate) were pretreated with anti-CD81 antibody (clone JS-81; BD Biosciences) or an isotype-matched control antibody (purified mouse IgG1, κ isotype control; BD Biosciences) as indicated for 1 h. Cells were then infected with the wild-type or mutant viruses at an m.o.i. of 0.5 or 0.01 for 6 h. The viruses were removed, and the cells were washed with PBS and then supplemented with complete DMEM. The efficiency of infection was monitored 1 day after infection by counting the number of HCV-positive foci by immunofluorescence.

Statistical analysis. A two-tailed Student's *t*-test was applied to evaluate the statistical significance of differences measured from the datasets. A *P* value of <0.05 was considered to be statistically significant.

RESULTS

Increase in HCV infectivity titres during serial passage

To produce infectious HCV particles, *in vitro*-transcribed genomic J6/JFH1 RNA was electroporated into Huh-7.5 cells. Transfected Huh-7.5 cells were maintained and the infectivity titre of the culture supernatant reached 6×10^4 f.f.u. ml^{-1} at 20 days post-infection. This culture supernatant was designated P-1.

To generate higher infectivity titres for HCV, naïve Huh-7.5 cells (3×10^5 cells per six-well plate) were infected with 1 ml virus stock of P-1 (6×10^4 f.f.u. ml^{-1}) at an m.o.i. of 0.2 and the infected cells were passaged serially every 3–4 days to maintain a subconfluent culture for 6 months. The culture medium was replaced with fresh complete DMEM every day. The extracellular infectivity titres fluctuated in the beginning after transfection and became lowest at the 22nd passage (Fig. 1a). Thereafter, the extracellular infectivity titres increased again and reached highest infectivity at the 47th passage. Therefore, we further examined the supernatants at the 27th, 38th and 47th passages, and the viruses were designated P-27, P-38 and P-47, respectively. The infectivity titres were determined to be 7.0×10^3 f.f.u. ml^{-1} for P-27, 1.7×10^4 f.f.u. ml^{-1} for P-38 and 3.3×10^4 f.f.u. ml^{-1} for P-47 (Fig. 1a). These viruses were used as inocula in the following experiments.

Kinetics of virus production after infection with putative adaptive J6/JFH1 mutants

To examine the virus-production kinetics of these viruses in Huh-7.5 cells, naïve Huh-7.5 cells (3×10^4 cells per 24-well plate) were infected with each inoculum (6×10^3 f.f.u.) at an m.o.i. of 0.2. After infection, the culture supernatants were harvested each day for 10 days and assayed for infectivity titres (Fig. 1b). The P-1 virus showed a peak infectivity titre of 2.3×10^4 f.f.u. ml^{-1} at 4 days post-infection, whereas the P-27, P-38 and P-47 viruses showed peak titres of 1.0×10^6, 2.3×10^6 and 6.0×10^6 f.f.u. ml^{-1} at 4–5 days post-infection, respectively (Fig. 1b), suggesting that these three viruses produce infectious HCV particles more efficiently than the P-1 virus. The increased infectivity titres may have been due to an increase in the absolute number of released HCV particles or an increased proportion of infectious relative to non-infectious particles. To address this question, we compared the specific infectivities of the mutant viruses with those of the wild-type virus. The ratio of viral infectivity titre (f.f.u. ml^{-1}) to HCV RNA content [genome equivalents (GE) ml^{-1}] was determined as shown in Table 1. The mutant viruses, P-27, P-38 and P-47, had higher specific-infectivity titres (1 : 21, 1 : 10 and 1 : 10, respectively) than the wild-type virus P-1 (1 : 133), suggesting that the mutant viruses are more infectious than the wild type and that the mutant viruses possess adaptive mutations in the virus genomes.

Sequence analysis of genetic mutations in the adaptive mutants

To identify the genetic changes in the virus genomes that are responsible for the adaptation to Huh-7.5 cells, we sequenced the whole genomes of the viruses. No mutation was found in the P-1 virus, whereas several mutations were identified in the P-27, P-38 and P-47 viruses (Fig. 1c). The sequencing analysis of P-27 identified eight mutations that were located in the E2, NS2, NS5A and NS5B regions as follows: T396A, T416A, N534H and A712V in E2; Y852H and W879R in NS2; F2281L in NS5A; and M2876L in NS5B (Fig. 1c). P-38 possessed 10 mutations, the same mutations as in P-27 and two additional mutations. The additional mutations were found at nucleotide position 146 (U to A) in the 5′-UTR and an amino acid change, K78E, in the core region. P-47 contained 11 mutations, including the same 10 mutations as P-38 and one additional mutation, T2925A in NS5B. Thus, the first eight mutations were all present in the genomes of the three viruses, and the results suggested that these eight mutations contribute to the enhanced infectivity.

Effects of individual mutations on the production of infectious HCV

To determine which mutation is responsible for the enhancement of infectivity, recombinant genomes containing only one of the selected mutations were constructed

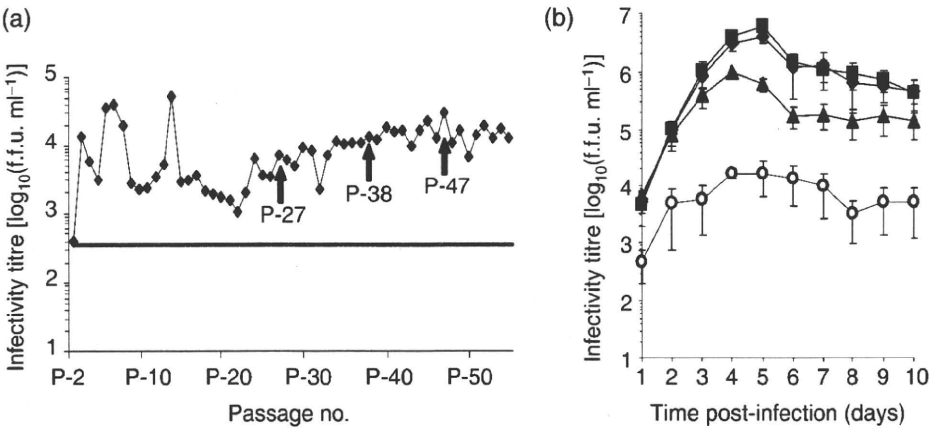

(c)

Virus	Position changed										
	5′-UTR	Core	E2				NS2		NS5A	NS5B	
	(nt 146)	78	396	416	534	712	852	879	2281	2876	2925
Wild-type	U	Lys	Thr	Thr	Asn	Ala	Tyr	Trp	Phe	Met	Thr
P-1	–	–	–	–	–	–	–	–	–	–	–
P-27	–	–	Ala	Ala	His	Val	His	Arg	Leu	Leu	–
P-38	A	Glu	Ala	Ala	His	Val	His	Arg	Leu	Leu	–
P-47	A	Glu	Ala	Ala	His	Val	His	Arg	Leu	Leu	Ala

Fig. 1. Increase in HCV infectivity titres during serial passage. (a) Serial passage of HCV J6/JFH1-infected Huh-7.5 cells. Huh-7.5 cells (3×10^5 cells per six-well plate) were infected with 1 ml stock of wild-type J6/JFH1 virus (P-1) (6×10^4 f.f.u. ml^{-1}) at an m.o.i. of 0.2, and the infected cells were passaged serially every 3–4 days to maintain a subconfluent culture for 6 months. The culture medium was replaced with fresh complete DMEM each day. The extracellular infectivity titres were determined by titration assay and are expressed as f.f.u. ml^{-1}. Arrows show the time points at which we collected the putative adapted viruses, designated P-27, P-38 and P-47. (b) Kinetics of virus production after infection with putative J6/JFH1 adaptive mutants in Huh-7.5 cells. Huh-7.5 cells were infected with the wild-type J6/JFH1 virus (○, P-1) or putative adaptive mutants (▲, P-27; ◆, P-38; ■, P-47) at an m.o.i. of 0.2. After infection, the culture supernatants were harvested every day until 10 days post-infection. Infectivity titres were measured by immunofluorescence assay and are expressed as f.f.u. ml^{-1}. Error bars represent SD for triplicate measurements. (c) Genetic mutations identified during passage. Numbers indicate the amino acid position where mutations were identified. The nucleotide position with mutation is given in parentheses.

(Fig. 2a). The *in vitro*-transcribed mutant J6/JFH1 RNAs were electroporated into Huh-7.5 cells and mutant viruses were generated. Then, naïve Huh-7.5 cells were infected with each virus at an m.o.i. of 0.01 and cultured for 12 days. The culture supernatant was collected every day from 1 to 12 days post-infection. The ability of each mutant virus to release infectious virus particles was examined by titration assay. As shown in Fig. 2(b), the recombinant viruses with single point mutations did not enhance the production of infectious virus particles, suggesting that a single point mutation is not enough for the enhanced infectivity.

Table 1. Specific-infectivity titres of the adaptive J6/JFH1 mutant viruses

Virus	HCV RNA copies [$\log_{10}$(GE ml^{-1})]	Infectivity titre [$\log_{10}$(f.f.u. ml^{-1})]	Specific infectivity (f.f.u. : GE)
P-1	6.7±0.1	4.6±0.1	1 : 133
P-27	7.3±0.1	6.0±0.2	1 : 21
P-38	7.4±0.1	6.4±0.0	1 : 10
P-47	7.3±0.1	6.3±0.2	1 : 10

Effects of combination of adaptive mutations on the production of infectious HCV

We then generated recombinant viruses with several mutations, as shown in Fig. 3(a). Naïve Huh-7.5 cells were infected with each virus at an m.o.i. of 0.01 and cultured for 12 days. The culture supernatant was collected every day from 1 to 12 days post-infection. The ability of each mutant virus to release infectious virus particles was examined by titration assay. The R-27, R-38 and R-47 viruses reached higher titres than the wild type and other mutant viruses, suggesting that all of the mutations in E2, NS2, NS5A and NS5B were important for the enhancement of infectivity (Fig. 3b). To determine the specific infectivities of the mutant viruses, the ratio of the viral infectivity titre (f.f.u. ml^{-1}) to the HCV RNA content (GE

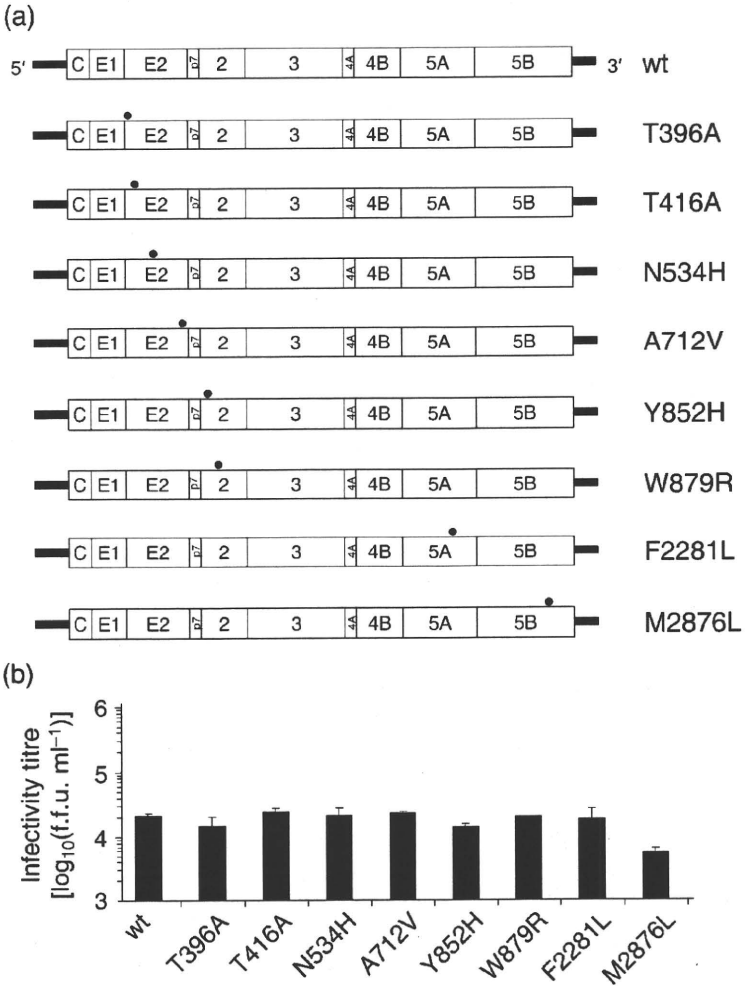

Fig. 2. Effects of individual mutations on the production of infectious HCV. (a) Schematic representation of the wild-type (wt) and mutant chimeric HCV J6/JFH1 genomes. HCV J6/JFH1 mutants with a single point mutation are shown. The adaptive mutations T396A, T416A, N534H, A712V, Y852H, W879R, F2281L and M2876L are indicated by ●. (b) The *in vitro*-transcribed mutant J6/JFH1 RNAs were electroporated into Huh-7.5 cells to generate recombinant mutant viruses. The infectivity titres of the culture supernatants were measured by titration assay. Then, naïve Huh-7.5 cells were infected with each virus at an m.o.i. of 0.01 and cultured for 12 days. The culture supernatant was collected every day from 1 to 12 days post-infection. The ability of each mutant virus to release infectious virus particles was examined by titration assay. Infectivity titres reached maximal levels at 10 days post-infection and the maximal infectivity titres were plotted. Error bars represent SD for triplicate measurements.

ml^{-1}) was calculated as shown in Table 2. The recombinant mutant viruses, R-27, R-38 and R-47, had higher specific-infectivity titres (1 : 46, 1 : 35 and 1 : 54, respectively) than the wild-type virus P-1 (1 : 197), suggesting that the particles released from cells infected with the R-27, R-38 and R-47 viruses are more infectious than those released from cells infected with the wild-type J6/JFH1 virus.

Efficient expression of HCV proteins in Huh-7.5 cells infected with the adaptive mutants

To investigate further the mechanism of adaptive mutations, we performed immunofluorescence staining of the infected cells. Huh-7.5 cells (6×10^4 cells per 24-well plate) were infected with the P-1, R-27, R-38 and R-47 viruses (1.2×10^4 f.f.u.) at an m.o.i. of 0.2. Cells were fixed 5 days post-infection and stained for immunofluorescence. Approximately 90 % of the cells were HCV-positive in the P-1-, R-27-, R-38- and R-47-infected cells (Fig. 4a). We next examined protein synthesis by immunoblotting for the HCV core and NS3 proteins. Immunoblot analysis of the cell lysates demonstrated that the levels of the core and NS3 proteins in cells infected with the R-27, R-38 and R-47 viruses were 2.0- to 2.5-fold higher than those in cells infected with the P-1 virus (Fig. 4b, c), suggesting that these mutant viruses have a replicative advantage.

Growth curves of infectious HCV after transfection of RNAs or infection with HCV

To determine whether the replicative advantage is at the level of entry or replication/translation of the genome, we examined one-step growth curves by transfecting equivalent amounts of RNAs of the wild-type and the mutant viruses into Huh-7.5 cells by means of electroporation (Fig. 5a, b). The intracellular and extracellular core protein levels were quantified by core protein-specific ELISA at the indicated times. The one-step growth curves showed that the intracellular and extracellular core protein levels increased with very similar kinetics in the cells transfected with the wild-type and adapted RNAs (Fig. 5a, b).

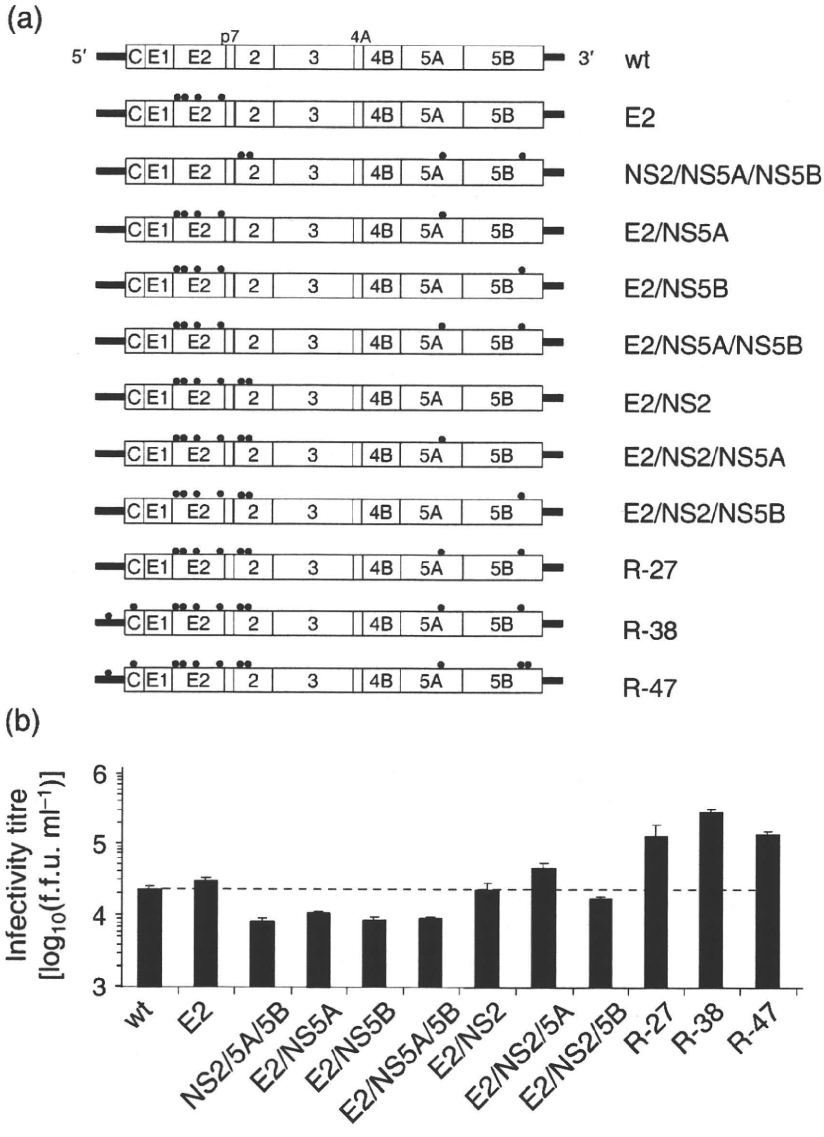

Fig. 3. Effects of combination of adaptive mutations on the production of infectious HCV. (a) Schematic representation of the wild-type (wt) and mutant chimeric HCV J6/JFH1 genomes. The HCV J6/JFH1 genomes with a combination of adaptive mutations at nt 146 (U to A) in the 5′-UTR and amino acid changes at K78E, T396A, T416A, N534H, A712V, Y852H, W879R, F2281L and M2876L are indicated by ●. (b) Recombinant mutant viruses with a combination of mutations were generated. Naïve Huh-7.5 cells were infected with each virus at an m.o.i. of 0.01 and cultured for 12 days. The ability of each mutant to release infectious virus particles was examined by titration assay. Infectivity titres reached maximal levels at 10 or 11 days post-infection and the maximal infectivity titres were plotted. Error bars represent SD for triplicate measurements.

We next examined the growth curves of the core protein levels by infecting cells with the recombinant viruses. The intracellular and extracellular core protein levels in cells infected with the P-1, R-27, R-38 and R-47 viruses were quantified. Huh-7.5 cells (1.2×10^5 cells per 12-well plate) were infected with these viruses at an m.o.i. of 0.2. The intracellular core protein levels in cells infected with the R-27, R-38 and R-47 viruses were 3- to 5-fold higher at day 1 post-infection than those in the P-1-infected cells. The intracellular core protein levels in the cells infected with the mutant viruses were 7- to 11-fold higher at day 3 post-infection than those in the P-1-infected cells (Fig. 5c). The extracellular core protein levels in the P-1-infected cells were comparable to the levels in cells infected with mutant viruses at day 1 post-infection. However, the extracellular core protein levels in cells infected with the R-27, R-38 and R-47 viruses increased more rapidly and reached 4.4- to 5.8-fold higher at day 3 post-infection than those in cells infected with the P-1 virus (Fig. 5d). Taken together, these data suggest that the adaptive mutants have advantages at the entry level, rather than the virus replication/translation level.

Table 2. Specific-infectivity titres of the recombinant adaptive mutant viruses

Virus	HCV RNA copies [$\log_{10}$(GE ml^{-1})]	Infectivity titre [$\log_{10}$(f.f.u. ml^{-1})]	Specific infectivity (f.f.u.:GE)
P-1	6.6±0.1	4.3±0.1	1:197
R-27	6.8±0.1	51±0.2	1:46
R-38	6.9±0	15.4±0.1	1:35
R-47	6.9±0.1	5.1±0.1	1:54

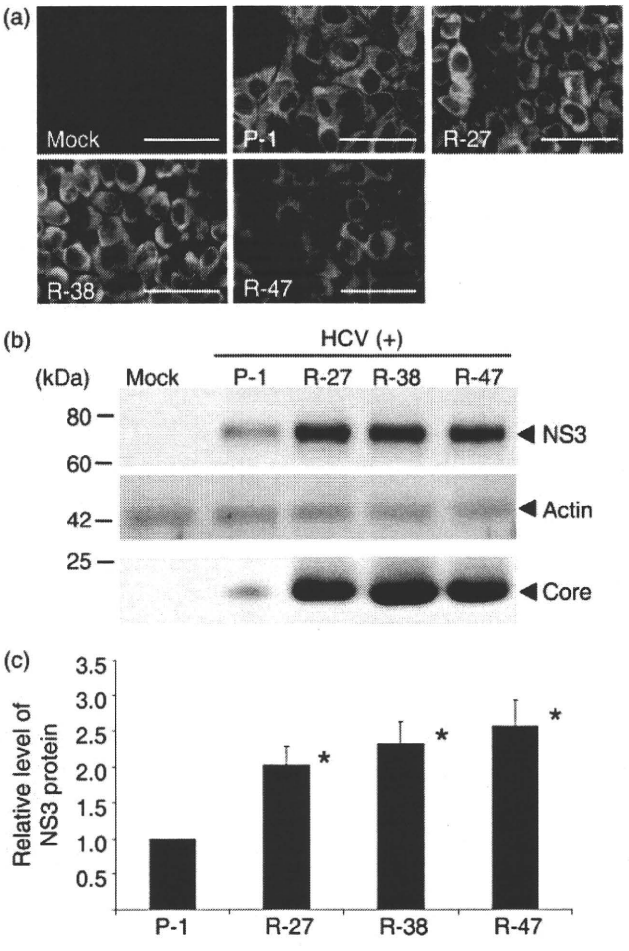

Fig. 4. Efficient expression of HCV proteins in Huh-7.5 cells infected with the adaptive mutants. Huh-7.5 cells (6×10^4 cells per 24-well plate) were infected with 200 µl P-1, R-27, R-38 or R-47 virus (6×10^4 f.f.u. ml^{-1}) at an m.o.i. of 0.2. (a) Cells were fixed 5 days post-infection and stained for immunofluorescence with anti-HCV-positive sera. Bars, 10 µm. (b) Immunoblot analysis of core and NS3 proteins in Huh-7.5 cells infected with R-27, R-38 and R-47 viruses. Data are representative of three independent experiments. (c) Quantification of the data shown in (b). Intensities of the gel bands were quantified by using the Scion Image for Windows program. The level of actin served as a loading control. Error bars represent SD for triplicate measurements. The difference between P-1 and the adaptive mutant (R-27, R-38 or R-47) was significant (*$P<0.05$ by Student's *t*-test).

Blocking of virus attachment and entry with anti-CD81 antibody

To determine whether the adapted mutant viruses have advantages at the entry level, we examined CD81-dependent entry into Huh-7.5 cells. Naïve Huh-7.5 cells were incubated with CD81-specific or non-specific antibody prior to inoculation. We scored infection by immunofluorescence at 24 h post-infection. As shown in Fig. 6(a), the anti-CD81 antibody inhibited the entry of the mutant viruses R-27, R-38 and R-47, as well as the wild-type virus, in a dose-dependent manner, suggesting that interaction between CD81 and HCV E2 glycoprotein is crucial for virus entry for all of these viruses. However, infections by the mutant viruses R-27, R-38 and R-47 were less dependent on CD81 than the wild-type virus. This result suggests that the mutations in the E2 glycoprotein confer an advantage to the mutant viruses at the entry level. We further analysed the mutant viruses to determine which mutation(s) is important for the advantage at the entry level. We infected Huh-7.5 cells with mutant viruses with a single point mutation in the E2 glycoprotein, such as T396A, T416A, N534H or A712V, or with all of the four mutations in E2. Blocking of virus entry with the anti-CD81 antibody was examined as shown in Fig. 6(b). Infection by the mutant virus N534H, as well as the mutant viruses E2, R-27, R-38 and R-47, was less dependent on CD81 than infection by the wild-type virus, whereas the other mutant viruses T396A, T416A and A712V showed a similar pattern to the wild type. These results indicate that the N534H mutation in the E2 region confers an advantage to the adaptive mutant viruses at the entry level.

DISCUSSION

In this study, we established an efficient HCV-production system by serial passaging of Huh-7.5 cells infected with the chimeric HCV J6/JFH1. Sequence analyses revealed that the adapted viruses possessed more than eight non-synonymous mutations in the genomes. Reverse-genetics analysis revealed that the recombinant viruses R-27, R-38 and R-47 exhibited higher expression of the HCV proteins than the wild-type virus. Moreover, we demonstrated that the N534H mutation in the E2 glycoprotein confers an advantage to the mutant viruses at the entry level.

The adaptive mutant viruses possessed four mutations (T396A, T416A, N534H and A712V) in E2. Two of these mutations (T416A and N534H) are in the regions that are involved in E2–CD81 binding and are, therefore, the possible target for neutralizing antibodies inhibiting E2–CD81 interactions (Helle & Dubuisson, 2008). The blocking of virus attachment and entry with CD81-specific antibody in this study revealed that the infections by the E2 R-27, R-38, R-47 and N534H mutants were less dependent on the CD81 molecule than that by the wild type J6/JFH1, suggesting that the N534H mutation gives the mutant viruses a selective advantage at the entry level. The N534H mutation is located in the sixth of 11 *N*-glycosylation sites, and is predicted to remove this *N*-glycosylation. The removal of *N*-glycosylation sites has been shown to have variable effects on CD81 binding and infectivity (Owsianka *et al.*, 2006; Roccasecca *et al.*, 2003). The glycans at positions 417, 532 and 645 (E2N1, E2N6 and E2N11) were shown to reduce the sensitivity of HCV pseudoparticles to antibody neutralization and to reduce the access of CD81 to its binding site on E2 (Goffard *et al.*, 2005). JFH-1 virus with the N534K mutation spread faster than the wild-type

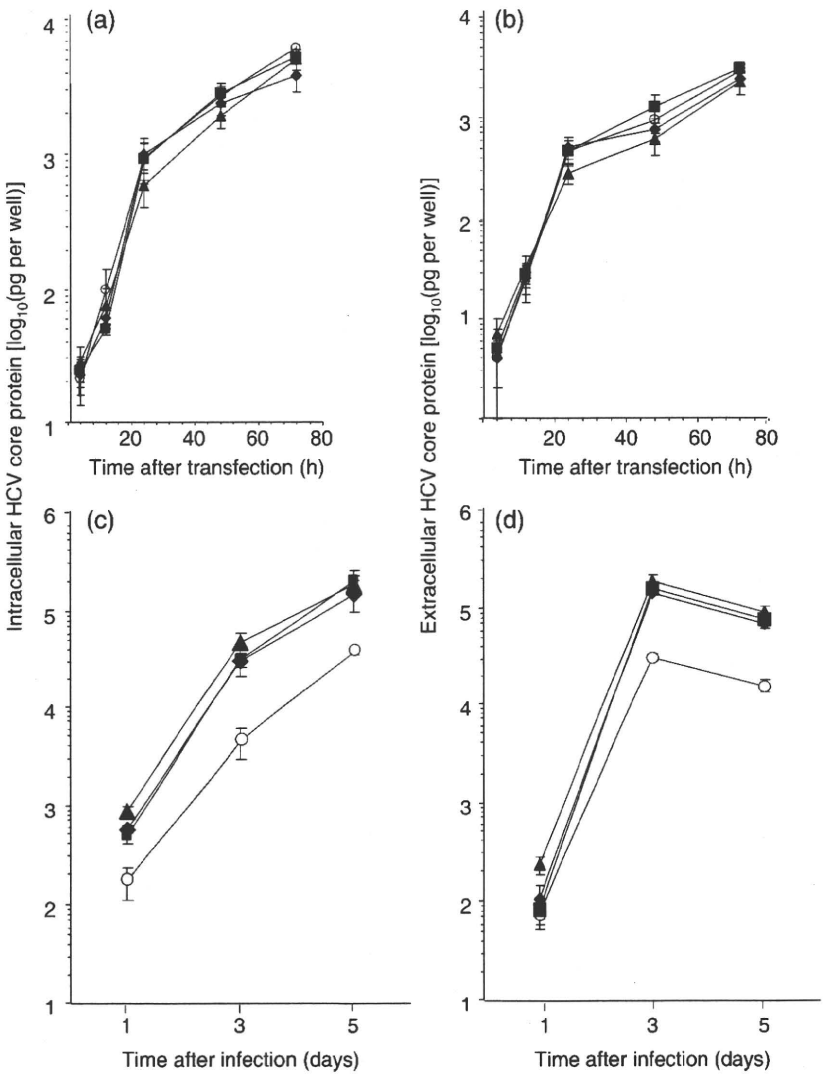

Fig. 5. Effects of adaptive mutations on the production of intracellular and extracellular core protein after transfection of *in vitro*-translated HCV RNAs or after infection of recombinant HCV. (a, b) After electroporation of 10 μg *in vitro*-translated HCV RNAs P-1 (○), R-27 (▲), R-38 (◆) and R-47 (■) into Huh-7.5 cells (5×10^6), the cells were divided into five sets, replated into a six-well plate and cultured. The cells and culture supernatants were harvested at the time points given. Intracellular (a) and extracellular (b) core protein levels were quantified by core protein-specific ELISA. (c, d) After Huh-7.5 cells (1.2×10^5 cells per 12-well plate) were infected with the P-1 (○), R-27 (▲), R-38 (◆) and R-47 (■) viruses at an m.o.i. of 0.2, the cells and culture supernatants were harvested at the time points given. Intracellular (c) and extracellular (d) core protein levels were quantified by core protein-specific ELISA.

JFH-1 virus after two successive amplifications in naïve cells, although the numbers of infectious viruses in the supernatant of transfected cells were initially low (Delgrange *et al.*, 2007). Our results in the growth curves of the viruses in the transfected cells and infected cells were consistent with their report. The CD81 inhibition assay in this study demonstrated clearly that the N534H mutation of the J6/JFH-1 virus confers a selective advantage for J6/JFH-1 at the entry level. To our knowledge, the present study is the first to prove that the mutation at site N534 gives infectious HCV a selective advantage at the entry level. These results raise two possibilities. One is that the N534H mutation in the E2 glycoprotein removes *N*-glycosylation and this mutant E2 glycoprotein possesses a higher affinity for the CD81 molecule, resulting in efficient entry to the cells. Another possibility is that the E2 glycoprotein with the N534H mutation gains higher affinity for other HCV receptors. Further investigation will be required to elucidate the mechanism of this adaptive mutation.

Our results showed that a combination of the mutations in E2, together with four additional mutations in NS2, NS5A and NS5B, resulted in higher infectivity of HCV, suggesting that the additional four mutations possess an advantage at different steps.

NS2 is a membrane-associated cysteine protease (Grakoui *et al.*, 1993; Hijikata *et al.*, 1993b; Lorenz *et al.*, 2006). The N terminus of NS2 consists of one or more transmembrane domains, whilst the C-terminal domain of NS2, together with the N-terminal one-third of NS3, forms the NS2–3 protease, an enzyme that catalyses a single cleavage at the NS2/NS3 boundary. The crystal structure of the C-terminal domain of NS2 has recently been determined and reveals a dimeric protease containing two composite active sites (Lorenz *et al.*, 2006). Jones *et al.* (2007) showed that NS2 and p7 are essential for HCV infectivity. The Y852 and W879 residues are located in the hydrophobic region of NS2. Although the exact topology of NS2 is disputed, the Y852H and W879R mutations would be predicted to lie

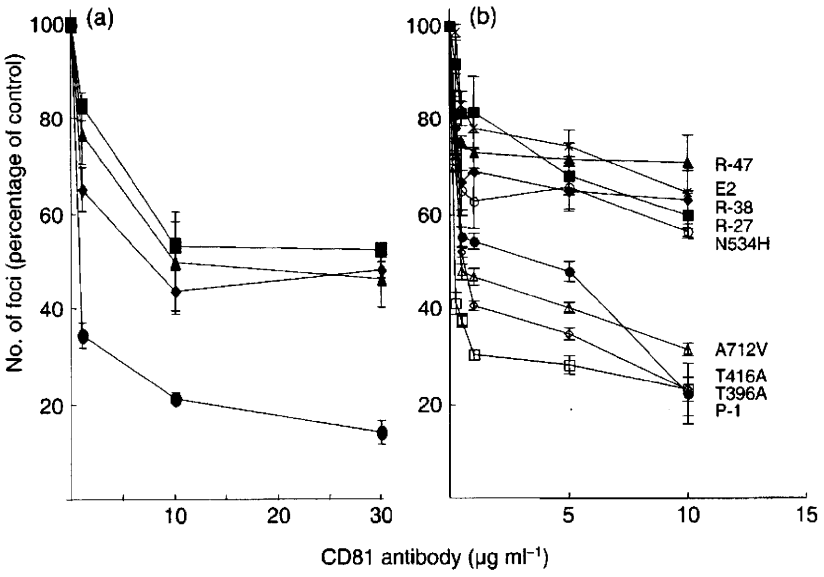

Fig. 6. Blocking of virus attachment and entry with anti-CD81 antibody. (a) Huh-7.5 cells (2×10^5 cells per six-well plate) were pretreated with 0, 1, 10 or 30 μg CD81 antibody (clone JS-81) ml^{-1} for 1 h and then infected with the wild-type (●, P-1) or recombinant mutant (■, R-27; ◆, R-38; ▲, R-47) viruses at an m.o.i. of 0.5. The cells were cultured for 24 h. The infection was monitored by HCV immunofluorescence and the numbers of HCV-positive foci were counted. Each result is expressed as a fraction of the number of foci observed in wells that received the control antibody instead of anti-CD81. Error bars represent SD for triplicate measurements. (b) Huh-7.5 cells (2×10^5 cells per six-well plate) were pretreated with 0, 0.25, 0.5, 1, 5 or 10 μg CD81 antibody ml^{-1} for 1 h and then infected with the wild-type (●, P-1) or recombinant (■, R-27; ◆, R-38; ▲, R-47; ×, E2; □, T396A; ◇, T416A; ○, N534H; △, A712V) viruses at an m.o.i. of 0.01. Blocking of virus entry with anti-CD81 antibody was examined. The infection was monitored by HCV immunofluorescence and the number of HCV-positive foci was counted.

within the second and third transmembrane domains, respectively (Yamaga & Ou, 2002). Murray *et al.* (2007) demonstrated that the A880P mutation increased infectious virus production significantly in the context of the J6/JFH1 genome, suggesting that the mutations in the transmembrane domain of NS2 play an important role in HCV infectivity. It is possible that the Y852H and W879R mutations in the transmembrane domain affect the topology and localization of NS2, and thereby HCV infectivity. Interestingly, NS2 has been found to interact with all other HCV NS proteins in *in vitro* pull-down assays, as well as cell-based colocalization and co-immunoprecipitation experiments (Dimitrova *et al.*, 2003; Hijikata *et al.*, 1993b), suggesting a role for NS2 as part of the replication complex.

Sequence analyses of HCV replicon cells revealed that highly adaptive mutations lie within the NS4B, NS5A and NS5B coding regions, with the majority clustering in NS5A. However, the mechanism underlying the replication enhancement is not known (Bartenschlager & Sparacio, 2007). The mutant viruses possessed an F2281L mutation that was located in domain II of NS5A. NS5A is an RNA-binding phosphoprotein composed of three domains that are separated by trypsin-sensitive low-complexity sequences (LCS I and LCS II) and an N-terminal amphipathic α-helix that anchors the protein stably to intracellular membranes (Brass *et al.*, 2002; Penin *et al.*, 2004; Tellinghuisen *et al.*, 2004). According to the X-ray crystal structure of domain I, it forms a dimer with a claw-like shape that can accommodate a single-stranded RNA molecule (Tellinghuisen *et al.*, 2005). Domain III of NS5A plays an important role in virus assembly and the production of infectious particles (Appel *et al.*, 2008; Masaki *et al.*, 2008; Tellinghuisen *et al.*, 2008). However, the role played by domain II of NS5A in the HCV replication cycle is unknown. Further examination will be required to clarify the effects of the F2281L mutation on the infectivity of the virus. Kaul *et al.* (2007) reported the V2941M mutation in NS5B in the context of the JFH1 genome. Lohmann *et al.* (2001) reported the R2884G mutation in the context of Con1-based replicon cells. Amino acid substitutions within NS5B may favour HCV replication and virus production in ways that remain to be determined.

Miyanari *et al.* (2007) proposed that HCV NS proteins and replication complexes are recruited to lipid droplet-associated membranes by the HCV core protein and that this recruitment is critical for producing infectious viruses. Cholesterol and sphingolipid associated with HCV particles are important for virion maturation and infectivity (Aizaki *et al.*, 2008). We speculate that the additional four mutations in NS2, NS5A and NS5B may confer an advantage in the maturation of virus particles or modification of virus envelopes with cholesterol and sphingolipid. Further investigation will be necessary to elucidate the mechanism of the adaptive mutations in NS2, NS5A and NS5B.

In conclusion, we have developed an efficient HCV-production system by passaging HCV J6/JFH1-infected Huh-7.5 cells. We have demonstrated that an efficient HCV-production system could be obtained by introducing adaptive mutations into the J6/JFH1 genome. The J6/JFH1-derived mutant viruses presented here would be a good tool for producing HCV particles with enhanced infectivity and for studying the molecular mechanism of HCV entry.

ACKNOWLEDGEMENTS

The authors are grateful to Dr C. M. Rice (Center for the Study of Hepatitis C, the Rockefeller University, New York, NY, USA) for providing pFL-J6/JFH1 and Huh-7.5 cells. This work was supported in part by grants-in-aid for Scientific Research from the Ministry of Education, Culture, Sports, Science and Technology (MEXT), and the Ministry of Health, Labour and Welfare, Japan. This study was also carried out as part of the Program of Founding Research Centers for Emerging and Reemerging Infectious Diseases, MEXT, Japan. This study was also part of the Global Center of Excellence (COE) Program at Kobe University Graduate School of Medicine.

REFERENCES

Aizaki, H., Morikawa, K., Fukasawa, M., Hara, H., Inoue, Y., Tani, H., Saito, K., Nishijima, M., Hanada, K. & other authors (2008). Critical role of virion-associated cholesterol and sphingolipid in hepatitis C virus infection. *J Virol* **82**, 5715–5724.

Appel, N., Zayas, M., Miller, S., Krijnse-Locker, J., Schaller, T., Friebe, P., Kallis, S., Engel, U. & Bartenschlager, R. (2008). Essential role of domain III of nonstructural protein 5A for hepatitis C virus infectious particle assembly. *PLoS Pathog* **4**, e1000035.

Bartenschlager, R. & Sparacio, S. (2007). Hepatitis C virus molecular clones and their replication capacity *in vivo* and in cell culture. *Virus Res* **127**, 195–207.

Bartosch, B., Vitelli, A., Granier, C., Goujon, C., Dubuisson, J., Pascale, S., Scarselli, E., Cortese, R., Nicosia, A. & Cosset, F. L. (2003). Cell entry of hepatitis C virus requires a set of co-receptors that include the CD81 tetraspanin and the SR-B1 scavenger receptor. *J Biol Chem* **278**, 41624–41630.

Blight, K. J., Kolykhalov, A. A. & Rice, C. M. (2000). Efficient initiation of HCV RNA replication in cell culture. *Science* **290**, 1972–1974.

Blight, K. J., McKeating, J. A. & Rice, C. M. (2002). Highly permissive cell lines for subgenomic and genomic hepatitis C virus RNA replication. *J Virol* **76**, 13001–13014.

Brass, V., Bieck, E., Montserret, R., Wolk, B., Hellings, J. A., Blum, H. E., Penin, F. & Moradpour, D. (2002). An amino-terminal amphipathic alpha-helix mediates membrane association of the hepatitis C virus nonstructural protein 5A. *J Biol Chem* **277**, 8130–8139.

Choo, Q. L., Kuo, G., Weiner, A. J., Overby, L. R., Bradley, D. W. & Houghton, M. (1989). Isolation of a cDNA clone derived from a blood-borne non-A, non-B viral hepatitis genome. *Science* **244**, 359–362.

Choo, Q. L., Richman, K. H., Han, J. H., Berger, K., Lee, C., Dong, C., Gallegos, C., Coit, D., Medina-Selby, R. & other authors (1991). Genetic organization and diversity of the hepatitis C virus. *Proc Natl Acad Sci U S A* **88**, 2451–2455.

Delgrange, D., Pillez, A., Castelain, S., Cocquerel, L., Rouille, Y., Dubuisson, J., Wakita, T., Duverlie, G. & Wychowski, C. (2007). Robust production of infectious viral particles in Huh-7 cells by introducing mutations in hepatitis C virus structural proteins. *J Gen Virol* **88**, 2495–2503.

Dimitrova, M., Imbert, I., Kieny, M. P. & Schuster, C. (2003). Protein-protein interactions between hepatitis C virus nonstructural proteins. *J Virol* **77**, 5401–5414.

Evans, M. J., von Hahn, T., Tscherne, D. M., Syder, A. J., Panis, M., Wolk, B., Hatziioannou, T., McKeating, J. A., Bieniasz, P. D. & Rice, C. M. (2007). Claudin-1 is a hepatitis C virus co-receptor required for a late step in entry. *Nature* **446**, 801–805.

Goffard, A., Callens, N., Bartosch, B., Wychowski, C., Cosset, F. L., Montpellier, C. & Dubuisson, J. (2005). Role of N-linked glycans in the functions of hepatitis C virus envelope glycoproteins. *J Virol* **79**, 8400–8409.

Gottwein, J. M., Scheel, T. K., Hoegh, A. M., Lademann, J. B., Eugen-Olsen, J., Lisby, G. & Bukh, J. (2007). Robust hepatitis C genotype 3a cell culture releasing adapted intergenotypic 3a/2a (S52/JFH1) viruses. *Gastroenterology* **133**, 1614–1626.

Grakoui, A., McCourt, D. W., Wychowski, C., Feinstone, S. M. & Rice, C. M. (1993). A second hepatitis C virus-encoded proteinase. *Proc Natl Acad Sci U S A* **90**, 10583–10587.

Helle, F. & Dubuisson, J. (2008). Hepatitis C virus entry into host cells. *Cell Mol Life Sci* **65**, 100–112.

Hijikata, M., Mizushima, H., Akagi, T., Mori, S., Kakiuchi, N., Kato, N., Tanaka, T., Kimura, K. & Shimotohno, K. (1993a). Two distinct proteinase activities required for the processing of a putative nonstructural precursor protein of hepatitis C virus. *J Virol* **67**, 4665–4675.

Hijikata, M., Mizushima, H., Tanji, Y., Komoda, Y., Hirowatari, Y., Akagi, T., Kato, N., Kimura, K. & Shimotohno, K. (1993b). Proteolytic processing and membrane association of putative nonstructural proteins of hepatitis C virus. *Proc Natl Acad Sci U S A* **90**, 10773–10777.

Jones, C. T., Murray, C. L., Eastman, D. K., Tassello, J. & Rice, C. M. (2007). Hepatitis C virus p7 and NS2 proteins are essential for production of infectious virus. *J Virol* **81**, 8374–8383.

Kaul, A., Woerz, I., Meuleman, P., Leroux-Roels, G. & Bartenschlager, R. (2007). Cell culture adaptation of hepatitis C virus and *in vivo* viability of an adapted variant. *J Virol* **81**, 13168–13179.

Kuo, G., Choo, Q. L., Alter, H. J., Gitnick, G. L., Redeker, A. G., Purcell, R. H., Miyamura, T., Dienstag, J. L., Alter, M. J. & other authors (1989). An assay for circulating antibodies to a major etiologic virus of human non-A, non-B hepatitis. *Science* **244**, 362–364.

Lindenbach, B. D., Evans, M. J., Syder, A. J., Wolk, B., Tellinghuisen, T. L., Liu, C. C., Maruyama, T., Hynes, R. O., Burton, D. R. & other authors (2005). Complete replication of hepatitis C virus in cell culture. *Science* **309**, 623–626.

Lohmann, V., Korner, F., Koch, J., Herian, U., Theilmann, L. & Bartenschlager, R. (1999). Replication of subgenomic hepatitis C virus RNAs in a hepatoma cell line. *Science* **285**, 110–113.

Lohmann, V., Korner, F., Dobierzewska, A. & Bartenschlager, R. (2001). Mutations in hepatitis C virus RNAs conferring cell culture adaptation. *J Virol* **75**, 1437–1449.

Lorenz, I. C., Marcotrigiano, J., Dentzer, T. G. & Rice, C. M. (2006). Structure of the catalytic domain of the hepatitis C virus NS2–3 protease. *Nature* **442**, 831–835.

Manns, M. P., Foster, G. R., Rockstroh, J. K., Zeuzem, S., Zoulim, F. & Houghton, M. (2007). The way forward in HCV treatment – finding the right path. *Nat Rev Drug Discov* **6**, 991–1000.

Masaki, T., Suzuki, R., Murakami, K., Aizaki, H., Ishii, K., Murayama, A., Date, T., Matsuura, Y., Miyamura, T., Wakita, T. & Suzuki, T. (2008). Interaction of hepatitis C virus nonstructural protein 5A with core

protein is critical for the production of infectious virus particles. *J Virol* **82**, 7964–7976.

McLauchlan, J., Lemberg, M. K., Hope, G. & Martoglio, B. (2002). Intramembrane proteolysis promotes trafficking of hepatitis C virus core protein to lipid droplets. *EMBO J* **21**, 3980–3988.

Miyanari, Y., Atsuzawa, K., Usuda, N., Watashi, K., Hishiki, T., Zayas, M., Bartenschlager, R., Wakita, T., Hijikata, M. & Shimotohno, K. (2007). The lipid droplet is an important organelle for hepatitis C virus production. *Nat Cell Biol* **9**, 1089–1097.

Muramatsu, S., Ishido, S., Fujita, T., Itoh, M. & Hotta, H. (1997). Nuclear localization of the NS3 protein of hepatitis C virus and factors affecting the localization. *J Virol* **71**, 4954–4961.

Murray, C. L., Jones, C. T., Tassello, J. & Rice, C. M. (2007). Alanine scanning of the hepatitis C virus core protein reveals numerous residues essential for production of infectious virus. *J Virol* **81**, 10220–10231.

Owsianka, A. M., Timms, J. M., Tarr, A. W., Brown, R. J., Hickling, T. P., Szwejk, A., Bienkowska-Szewczyk, K., Thomson, B. J., Patel, A. H. & Ball, J. K. (2006). Identification of conserved residues in the E2 envelope glycoprotein of the hepatitis C virus that are critical for CD81 binding. *J Virol* **80**, 8695–8704.

Penin, F., Brass, V., Appel, N., Ramboarina, S., Montserret, R., Ficheux, D., Blum, H. E., Bartenschlager, R. & Moradpour, D. (2004). Structure and function of the membrane anchor domain of hepatitis C virus nonstructural protein 5A. *J Biol Chem* **279**, 40835–40843.

Pietschmann, T., Lohmann, V., Kaul, A., Krieger, N., Rinck, G., Rutter, G., Strand, D. & Bartenschlager, R. (2002). Persistent and transient replication of full-length hepatitis C virus genomes in cell culture. *J Virol* **76**, 4008–4021.

Pileri, P., Uematsu, Y., Campagnoli, S., Galli, G., Falugi, F., Petracca, R., Weiner, A. J., Houghton, M., Rosa, D. & other authors (1998). Binding of hepatitis C virus to CD81. *Science* **282**, 938–941.

Poynard, T., Yuen, M. F., Ratziu, V. & Lai, C. L. (2003). Viral hepatitis C. *Lancet* **362**, 2095–2100.

Roccasecca, R., Ansuini, H., Vitelli, A., Meola, A., Scarselli, E., Acali, S., Pezzanera, M., Ercole, B. B., McKeating, J. & other authors (2003). Binding of the hepatitis C virus E2 glycoprotein to CD81 is strain specific and is modulated by a complex interplay between hypervariable regions 1 and 2. *J Virol* **77**, 1856–1867.

Russell, R. S., Meunier, J. C., Takikawa, S., Faulk, K., Engle, R. E., Bukh, J., Purcell, R. H. & Emerson, S. U. (2008). Advantages of a single-cycle production assay to study cell culture-adaptive mutations of hepatitis C virus. *Proc Natl Acad Sci U S A* **105**, 4370–4375.

Saito, I., Miyamura, T., Ohbayashi, A., Harada, H., Katayama, T., Kikuchi, S., Watanabe, Y., Koi, S., Onji, M. & other authors (1990). Hepatitis C virus infection is associated with the development of hepatocellular carcinoma. *Proc Natl Acad Sci U S A* **87**, 6547–6549.

Scarselli, E., Ansuini, H., Cerino, R., Roccasecca, R. M., Acali, S., Filocamo, G., Traboni, C., Nicosia, A., Cortese, R. & Vitelli, A. (2002). The human scavenger receptor class B type I is a novel candidate receptor for the hepatitis C virus. *EMBO J* **21**, 5017–5025.

Schaller, T., Appel, N., Koutsoudakis, G., Kallis, S., Lohmann, V., Pietschmann, T. & Bartenschlager, R. (2007). Analysis of hepatitis C virus superinfection exclusion by using novel fluorochrome gene-tagged viral genomes. *J Virol* **81**, 4591–4603.

Sumpter, R., Jr, Loo, Y. M., Foy, E., Li, K., Yoneyama, M., Fujita, T., Lemon, S. M. & Gale, M., Jr (2005). Regulating intracellular antiviral defense and permissiveness to hepatitis C virus RNA replication through a cellular RNA helicase, RIG-I. *J Virol* **79**, 2689–2699.

Takigawa, Y., Nagano-Fujii, M., Deng, L., Hidajat, R., Tanaka, M., Mizuta, H. & Hotta, H. (2004). Suppression of hepatitis C virus replicon by RNA interference directed against the NS3 and NS5B regions of the viral genome. *Microbiol Immunol* **48**, 591–598.

Tellinghuisen, T. L., Marcotrigiano, J., Gorbalenya, A. E. & Rice, C. M. (2004). The NS5A protein of hepatitis C virus is a zinc metalloprotein. *J Biol Chem* **279**, 48576–48587.

Tellinghuisen, T. L., Marcotrigiano, J. & Rice, C. M. (2005). Structure of the zinc-binding domain of an essential component of the hepatitis C virus replicase. *Nature* **435**, 374–379.

Tellinghuisen, T. L., Foss, K. L., Treadaway, J. C. & Rice, C. M. (2008). Identification of residues required for RNA replication in domains II and III of the hepatitis C virus NS5A protein. *J Virol* **82**, 1073–1083.

Wakita, T., Pietschmann, T., Kato, T., Date, T., Miyamoto, M., Zhao, Z., Murthy, K., Habermann, A., Krausslich, H. G. & other authors (2005). Production of infectious hepatitis C virus in tissue culture from a cloned viral genome. *Nat Med* **11**, 791–796.

Yamaga, A. K. & Ou, J. H. (2002). Membrane topology of the hepatitis C virus NS2 protein. *J Biol Chem* **277**, 33228–33234.

Yi, M., Villanueva, R. A., Thomas, D. L., Wakita, T. & Lemon, S. M. (2006). Production of infectious genotype 1a hepatitis C virus (Hutchinson strain) in cultured human hepatoma cells. *Proc Natl Acad Sci U S A* **103**, 2310–2315.

Yi, M., Ma, Y., Yates, J. & Lemon, S. M. (2007). Compensatory mutations in E1, p7, NS2, and NS3 enhance yields of cell culture-infectious intergenotypic chimeric hepatitis C virus. *J Virol* **81**, 629–638.

Zhong, J., Gastaminza, P., Cheng, G., Kapadia, S., Kato, T., Burton, D. R., Wieland, S. F., Uprichard, S. L., Wakita, T. & Chisari, F. V. (2005). Robust hepatitis C virus infection *in vitro*. *Proc Natl Acad Sci U S A* **102**, 9294–9299.

Zhong, J., Gastaminza, P., Chung, J., Stamataki, Z., Isogawa, M., Cheng, G., McKeating, J. A. & Chisari, F. V. (2006). Persistent hepatitis C virus infection *in vitro*: coevolution of virus and host. *J Virol* **80**, 11082–11093.

JOURNAL OF VIROLOGY, Nov. 2008, p. 10375–10385 Vol. 82, No. 21
0022-538X/08/$08.00+0 doi:10.1128/JVI.00395-08

Hepatitis C Virus Infection Induces Apoptosis through a Bax-Triggered, Mitochondrion-Mediated, Caspase 3-Dependent Pathway▽

Lin Deng,[1] Tetsuya Adachi,[1] Kikumi Kitayama,[1] Yasuaki Bungyoku,[1] Sohei Kitazawa,[2] Satoshi Ishido,[3] Ikuo Shoji,[1] and Hak Hotta[1]*

Divisions of Microbiology[1] and Molecular Pathology,[2] Kobe University Graduate School of Medicine, 7-5-1 Kusunoki-cho, Chuo-ku, Kobe 650-0017, and Laboratory for Infectious Immunity, Riken Research Center for Allergy and Immunology, 1-7-22 Suehiro-cho, Tsurumi-ku, Yokohama, Kanagawa 230-0045,[3] Japan

Received 23 February 2008/Accepted 20 August 2008

We previously reported that cells harboring the hepatitis C virus (HCV) RNA replicon as well as those expressing HCV NS3/4A exhibited increased sensitivity to suboptimal doses of apoptotic stimuli to undergo mitochondrion-mediated apoptosis (Y. Nomura-Takigawa, et al., J. Gen. Virol. 87:1935–1945, 2006). Little is known, however, about whether or not HCV infection induces apoptosis of the virus-infected cells. In this study, by using the chimeric J6/JFH1 strain of HCV genotype 2a, we demonstrated that HCV infection induced cell death in Huh7.5 cells. The cell death was associated with activation of caspase 3, nuclear translocation of activated caspase 3, and cleavage of DNA repair enzyme poly(ADP-ribose) polymerase, which is known to be an important substrate for activated caspase 3. These results suggest that HCV-induced cell death is, in fact, apoptosis. Moreover, HCV infection activated Bax, a proapoptotic member of the Bcl-2 family, as revealed by its conformational change and its increased accumulation on mitochondrial membranes. Concomitantly, HCV infection induced disruption of mitochondrial transmembrane potential, followed by mitochondrial swelling and release of cytochrome *c* from mitochondria. HCV infection also caused oxidative stress via increased production of mitochondrial superoxide. On the other hand, HCV infection did not mediate increased expression of glucose-regulated protein 78 (GRP78) or GRP94, which are known as endoplasmic reticulum (ER) stress-induced proteins; this result suggests that ER stress is not primarily involved in HCV-induced apoptosis in our experimental system. Taken together, our present results suggest that HCV infection induces apoptosis of the host cell through a Bax-triggered, mitochondrion-mediated, caspase 3-dependent pathway(s).

Hepatitis C virus (HCV) often establishes persistent infection to cause chronic hepatitis, liver cirrhosis, and hepatocellular carcinoma, which is a significant health problem around the world (56). Although the exact mechanisms of HCV pathogenesis, such as viral persistence, liver cell injury, and carcinogenesis, are not fully understood yet, an accumulating body of evidence suggests that apoptosis of hepatocytes is significantly involved in the pathogenesis of HCV (1, 2, 9). It is widely accepted that apoptosis of virus-infected cells is an important strategy of the host to protect itself against viral infections. Apoptotic cell death can be mediated either by the host immune responses through the function of virus-specific cytotoxic T lymphocytes and/or by viral proteins themselves that trigger an apoptotic pathway(s) of the host cell.

Apoptotic pathways can be classified into two groups: the mitochondrial death (intrinsic) pathway and the extrinsic cell death pathway initiated by the tumor necrosis factor (TNF) family members (31, 63). Mitochondrion-mediated apoptosis is initiated by a variety of apoptosis-inducing signals that cause the imbalance of the major apoptosis regulator, the proteins of the Bcl-2 family, such as Bcl-2, Bax, and Bid. For example, the proapoptotic protein Bax accumulates on mitochondria after being activated and triggers an increase in the permeability of the outer mitochondrial membrane. Consequently, the mitochondria release cytochrome *c* and other key molecules that facilitate apoptosome formation to activate caspase 9. This, in turn, activates downstream death programs, such as caspase 3 and poly(ADP-ribose) polymerase (PARP). The mitochondria also release apoptosis-inducing factor and endonuclease G to facilitate caspase-independent apoptosis. On the other hand, the extrinsic cell death pathway involves the activation of caspase 8 through binding to the adaptor protein Fas-associated protein with death domain (FADD), which in turn activates caspase 3 to facilitate cell death.

There have been many studies regarding the HCV protein(s) that is directly involved in apoptosis, identifying the protein as either proapoptotic or antiapoptotic, and some data are inconsistent. For example, core (5, 13, 36, 73), E1 (15, 16), E2 (12), NS3 (48), NS4A (43), and NS5A and NS5B (57) have been reported to induce apoptosis. On the other hand, there are reports showing that core (40, 49, 51), E2 (35), NS2 (21), NS3 (58), and NS5A (33, 67) function as antiapoptotic proteins. However, whether the virus as a whole is proapoptotic or antiapoptotic needs to be studied in the context of virus replication, which is believed to be much more dynamic than mere expression of a viral protein(s).

We previously reported that replication of an HCV RNA replicon rendered the host cell prone to undergoing mitochondrion-mediated apoptosis upon suboptimal doses of apoptosis-inducing stimuli (43). Recently, an efficient virus infection system using a particular clone of HCV genotype 2a and a highly permissive human hepatocellular carcinoma-derived cell line

* Corresponding author. Mailing address: Division of Microbiology, Kobe University Graduate School of Medicine, 7-5-1 Kusunoki-cho, Chuo-ku, Kobe 650-0017, Japan. Phone: 81-78-382-5500. Fax: 81-78-382-5519. E-mail: hotta@kobe-u.ac.jp.

▽ Published ahead of print on 3 September 2008.

has been developed (37, 38, 66, 71). In this study, by using the virus infection system, we examined the possible effect of HCV infection on the fate of the host cell. We report here that HCV infection induces apoptosis via the mitochondrion-mediated pathway, as demonstrated by the increased accumulation of the proapoptotic protein Bax on the mitochondria, decreased mitochondrial transmembrane potential, and mitochondrial swelling, which result in the release of cytochrome *c* from the mitochondria and the activation of caspase 3.

MATERIALS AND METHODS

Cells. The Huh7.5 cell line (6), a highly HCV-susceptible subclone of Huh7 cells, was a kind gift from C. M. Rice, Center for the Study of Hepatitis C, The Rockefeller University. The cells were propagated in Dulbecco's modified Eagle medium supplemented with 10% heat-inactivated fetal bovine serum and 0.1 mM nonessential amino acids.

Virus. The virus stock used in this study was prepared as described below. The pFL-J6/JFH1 plasmid, encoding the entire viral genome of a chimeric strain of HCV genotype 2a, J6/JFH1 (37), was kindly provided by C. M. Rice. The plasmid was linearized by XbaI digestion and in vitro transcribed by using T7 RiboMAX (Promega, Madison, WI) to generate the full-length viral genomic RNA. The in vitro-transcribed RNA (10 μg) was transfected into Huh7.5 cells by means of electroporation (975 μF, 270 V) using Gene Pulser (Bio-Rad, Hercules, CA). The cells were then cultured in complete medium, and the supernatant was propagated as an original virus (J6/JFH1-passage 1 [J6/JFH1-P1]). Since the infectious titer of the original virus was not high enough for infection of all the cells in the culture at once, an adapted strain of the virus was obtained by passaging the virus-infected cells 47 times. The adapted virus (J6/JFH1-P47), which is a pool of adapted mutants, possesses 10 amino acid mutations (K78E, T396A, T416A, N534H, A712V, Y852H, W879R, F2281L, M2876L, and T2925A) and a single nucleotide mutation in the 5′-untranslated region (U146A) and produces a much higher titer of infectivity in Huh7.5 cell cultures than the original J6/JFH1-P1 (our unpublished data). Virus infection was performed at a multiplicity of infection of 2.0. Culture supernatants of uninfected cells served as a control (mock preparation).

Virus infectivity was measured by indirect immunofluorescence analysis, as described below, and expressed as cell-infecting units/ml.

Cell viability/proliferation assay. Huh7.5 cells were seeded in 96-well plates at a density of 1.0×10^4 cells/well and cultured overnight. The cells were then infected with the virus or the mock preparation, and, at different time points, cell viability/proliferation was determined by the WST-1 assay (Roche, Mannheim, Germany), as described previously (43).

Detection of apoptosis. The degree of apoptosis was measured by using a Cell Death Detection ELISA^{Plus} kit (Roche), which is based on the determination of cytoplasmic histone-associated DNA fragments, according to the manufacturer's protocol. In brief, cells cultured in a 96-well plate were centrifuged at $200 \times g$ for 10 min at 4°C to remove the supernatant. After the cells were lysed with lysis buffer, the plate was centrifuged at $200 \times g$ for 10 min to separate the cytoplasmic and nuclear fractions. Twenty microliters of supernatant was placed in each well of a streptavidin-coated 96-well plate. Subsequently, a mixture of biotin-labeled anti-histone antibody and peroxidase-labeled anti-DNA antibody was added and wells were incubated for 2 h at room temperature. After wells were washed three times to remove the unbound components, peroxidase activities were determined photometrically with 2,2′-azino-diethyl-benzthiazolin sulfonate as a substrate and measured by using a microplate reader (Bio-Rad).

Caspase enzymatic activities. Activities of caspase 3, 8, and 9 were measured by using Caspase-Glo 3/7, 8, and 9 assays (Promega), respectively, according to the manufacturer's instructions. In brief, a proluminescence caspase 3/7, 8, or 9 substrate, which consists of aminoluciferin (substrate for luciferase) and the tetrapeptide sequence DEVD, LETD, or LEHD (cleavage site for caspase 3/7, 8, or 9, respectively), was added to cultured cells in each well of a 96-well plate, and the plate was incubated for 30 min at room temperature. In the presence of caspase 3/7, 8, or 9, aminoluciferin was liberated from the proluminescence substance and utilized as a substrate for the luciferase reaction. The resultant luminescence in relative light units was measured by using a Luminescencer-JNR AB-2100 (Atto, Tokyo, Japan).

Cell fractionation. Cells were fractionated by using a mitochondrial isolation kit (Pierce, Rockford, IL), according to the manufacturer's instructions. Briefly, 2×10^7 cells were harvested and suspended in reagent A containing a protease inhibitor cocktail (Roche). The cell suspension was mixed with buffer B, vortexed for 5 min, and then mixed with reagent C. The nuclei and unbroken cells were removed by centrifugation at $700 \times g$ for 10 min at 4°C, and the supernatant was used as cell lysate. The cell lysate was further centrifuged at $3,000 \times g$ for 15 min at 4°C. The pellet obtained, which was considered the mitochondrial fraction, was washed once with reagent C and dissolved in a lysis buffer containing 10 mM Tris-HCl (pH 7.5), 150 mM NaCl, 1 mM EDTA, 1% NP-40, and a protease inhibitor cocktail. The remaining supernatant was further centrifuged at $100,000 \times g$ for 30 min at 4°C, and the resultant supernatant was collected as a cytosolic fraction.

To verify successful mitochondrial fractionation, the cytosolic and mitochondrial fractions were analyzed by immunoblotting, as described below, using antibody against Tim23, a mitochondrion-specific protein.

Analysis of the mitochondrial transmembrane potential. The mitochondrial transmembrane potential was measured by flow cytometry using the cationic lipophilic green fluorochrome rhodamine 123 (Rho123; Sigma, St. Louis, MO), as described previously (43). Briefly, cells (7×10^5) were harvested, washed twice with phosphate-buffered saline (PBS), and incubated with Rho123 (0.5 μg/ml) at 37°C for 25 min. The cells were then washed twice with PBS, and Rho123 intensity was analyzed by a flow cytometer (Becton Dickinson, San Jose, CA). A total of 10,000 events were collected per sample. Mean fluorescence intensities were measured by calculating the geometric mean for each histogram peak.

Detection of morphological changes of the mitochondria. Mitochondrial morphology was analyzed by two different methods. (i) For fluorescence microscopy, Huh7.5 cells seeded on glass coverslips in a 24-well plate were incubated for 30 min at 37°C with 100 nM MitoTracker (Molecular Probes, Eugene, OR). After being washed twice with PBS, the cells were fixed with 3.7% paraformaldehyde and observed under a confocal laser scanning microscope (Carl Zeiss, Oberkochen, Germany). When needed, the fixed cells were subjected to indirect immunofluorescence to confirm HCV infection, as described below. (ii) Electron microscopy was performed as described previously (23, 43). In brief, cells were fixed with 4% paraformaldehyde and 0.2% glutaraldehyde for 30 min at room temperature. After being washed with PBS, the cells were collected, dehydrated in a series of 70%, 80%, and 90% ethanol, embedded in LR White resin (London Resin, Berkshire, United Kingdom), and kept at −20°C for 2 days to facilitate resin polymerization. After ultrathin sectioning, samples were etched in 3% H_2O_2 for 5 min at room temperature and washed with PBS. Sections were stained with uranyl acetate and lead citrate and observed under a transmission electron microscope (JEM 1299EX; JOEL, Tokyo, Japan).

Detection of mitochondrial superoxide. Cells seeded on glass coverslips in a 24-well plate were incubated with 5 μM MitoSOX Red (Molecular Probes) at 37°C for 10 min. After being washed with warm Hanks' balanced salt solution with calcium and magnesium (Invitrogen, Carlsbad, CA), the cells were fixed with 3.7% paraformaldehyde and observed under a confocal laser scanning microscope (Carl Zeiss). When needed, the fixed cells were subjected to indirect immunofluorescence to confirm HCV infection, as described below.

Indirect immunofluorescence. Cells seeded on glass coverslips in a 24-well plate at a density of 6×10^4 cells/well were infected with HCV or left uninfected. At different time points after virus infection, the cells were fixed with 3.7% paraformaldehyde in PBS for 15 min at room temperature and permeabilized in 0.1% Triton X-100 in PBS for 15 min at room temperature. After being washed with PBS twice, cells were consecutively stained with primary and secondary antibodies. Primary antibodies used were anti-active caspase 3 rabbit polyclonal antibody (Promega) and an HCV-infected patient's serum. Secondary antibodies used were Cy3-conjugated donkey anti-rabbit immunoglobulin G (IgG; Chemicon, Temecula, CA), Alexa Fluor 594-conjugated goat anti-human IgG (Molecular Probes), and fluorescein isothiocyanate (FITC)-conjugated goat anti-human IgG (MBL, Nagoya, Japan). The cells were washed with PBS, counterstained with Hoechst 33342 solution (Molecular Probes) at room temperature for 10 min, mounted on glass slides, and observed under a confocal laser scanning microscope (Carl Zeiss). The specificity of this immunostaining was confirmed by using mouse monoclonal antibody against HCV core protein (C7-50; Abcam, Tokyo, Japan).

To analyze the possible localization of the activated Bax on mitochondrial membranes, cells were incubated with MitoTracker and subjected to immunofluorescence analysis using rabbit polyclonal antibody against activated Bax (NT antibody; Upstate, Lake Placid, NY). This antibody is directed toward N-terminal residues 1 to 21 of Bax in an N-terminal conformation-dependent manner and specifically recognizes the active form of Bax, in which this segment is exposed in response to apoptotic stimuli (64).

Immunoblotting. Cells were lysed in a buffer containing 10 mM Tris-HCl (pH 7.5), 150 mM NaCl, 1 mM EDTA, 1% NP-40, and a protease inhibitor cocktail (Roche). After two freeze-thaw cycles, cell debris was removed by

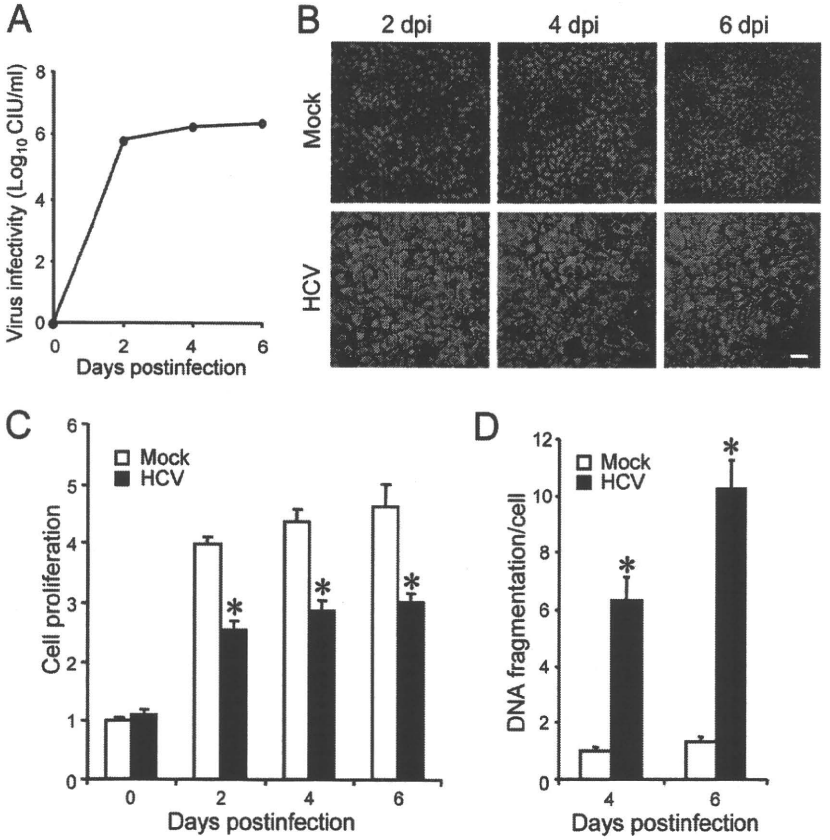

FIG. 1. HCV infection induces apoptosis in Huh7.5 cells. (A) Virus infectivity in the culture supernatants of HCV-infected cells. (B) Detection of HCV antigens in the cells. Huh7.5 cells mock inoculated or inoculated with HCV were subjected to indirect immunofluorescence analysis to detect HCV antigens (red staining) using an HCV-infected patient's serum and Alexa Fluor 594-conjugated goat anti-human IgG at 2, 4, and 6 days postinfection (dpi). Nuclei were counterstained with Hoechst 33342 (blue staining). Scale bar, 50 μm. (C) Cell viability/proliferation was measured for HCV-infected cultures and the mock-inoculated controls. Proliferation of the control cells at day 0 postinfection was arbitrarily expressed as 1.0. Data represent means ± standard deviations (SD) of three independent experiments. *, $P < 0.01$, compared with the control. (D) DNA fragmentation was measured as an index of apoptotic cell death for HCV-infected cultures and the mock-inoculated controls. DNA fragmentation of the control cells at 4 days postinfection was arbitrarily expressed as 1.0. Data represent means ± SD of three independent experiments. *, $P < 0.01$, compared with the control.

centrifugation. Protein quantification was carried out using a bicinchoninic acid protein assay kit (Pierce). Equal amounts of soluble proteins (4 to 20 μg) were subjected to sodium dodecyl sulfate-polyacrylamide gel electrophoresis and transferred onto a polyvinylidene difluoride membrane (Millipore, Bedford, MA), which was then incubated with the respective primary antibody. The primary antibodies used were mouse monoclonal antibodies against cytochrome *c* (A-8; Santa Cruz Biotechnology, Santa Cruz, CA), HCV NS3 (Chemicon), Tim23, Bax and Bcl-2 (BD Biosciences Pharmingen, San Diego, CA); rabbit polyclonal antibodies against Bak (Upstate), caspase 3, and PARP (Cell Signaling Technology, Danvers, MA); and goat polyclonal antibodies against glucose-regulated protein 78 (GRP78) and GRP94 (Santa Cruz Biotechnology). Horseradish peroxidase-conjugated goat anti-mouse IgG (MBL), goat anti-rabbit IgG (Bio-Rad), and donkey anti-goat IgG (Santa Cruz Biotechnology) were used as secondary antibodies. In some experiments, a commercial kit that facilitates the antigen-antibody reaction (Can Get Signal; Toyobo, Osaka, Japan) was used to obtain stronger signals. The respective protein bands were visualized by means of an enhanced chemiluminescence (GE Healthcare, Buckinghamshire, United Kingdom), and the intensity of each band was quantified by using NIH Image J. Protein loading was normalized by probing with goat antibody against actin (Santa Cruz Biotechnology) as a primary antibody.

Statistical analysis. The two-tailed Student *t* test was applied to evaluate the statistical significance of differences measured from the data sets. A *P* value of <0.05 was considered statistically significant.

RESULTS

HCV infection induces caspase 3-dependent apoptosis in Huh7.5 cells. We first examined virus growth in Huh7.5 cells. HCV grew efficiently in the culture, and virus titers in the supernatant reached a plateau level at 2 days postinfection (Fig. 1A). Immunofluorescence analysis revealed that >95% of the cells were infected with HCV on the same day (Fig. 1B). To examine the possible impact of HCV infection on the cells, we measured the cell viability/proliferation at 0, 2, 4, and 6 days postinfection. As shown in Fig. 1C, the proliferation of HCV-infected cells was significantly slower than that of the mock-infected control. Similar results were obtained when the parental Huh7 cells were used for HCV infection (data not shown). The observed delay in cell proliferation was associated with an increase in cell death, seen as cell rounding and floating in the culture (data not shown) and in cellular DNA fragmentation (Fig. 1D). As DNA fragmentation is a hallmark of apoptosis, our data suggest that HCV infection induces apoptosis in Huh7.5 cells.

The J6/JFH1-P47 strain of HCV used in this study possesses adaptive mutations compared to the original strain (J6/JFH1-P1). Therefore, we compared the impacts of the two strains on cell viability/proliferation and DNA fragmentation. While both strains caused inhibition of cell proliferation and an increase in DNA fragmentation, J6/JFH1-P47 appeared to exert a stronger cytopathic effect than J6/JFH-P1 (data not shown).

To further verify that HCV infection induces apoptotic cell death, we analyzed caspase 3 activities in HCV-infected Huh7.5 cells and the mock-infected control. As shown in Fig. 2A, caspase 3 activities in HCV-infected cells increased to levels that were 2.2, 6.0, and 12 times higher than that in the control cells at 2, 4, and 6 days postinfection, respectively. We also examined HCV-induced caspase 3 activation by immunoblot analysis. Activation of caspase 3 requires proteolytic processing of its inactive proenzyme into the active 17-kDa and 12-kDa subunit proteins. The anti-caspase 3 antibody used in this analysis recognizes 35-kDa procaspase 3 and the 17-kDa subunit protein. At 6 days postinfection, activated caspase 3 was detected in HCV-infected cells but not in the mock-infected control (Fig. 2B, second row from the top). Analysis of the death substrate PARP, which is a key substrate for active caspase 3 (61), also demonstrated that the uncleaved PARP (116 kDa) was proteolytically cleaved to generate the 89-kDa fragment in HCV-infected cells but not in the mock-infected control (Fig. 2B, third row). Cleavage of PARP facilitates cellular disassembly and serves as a marker of cells undergoing apoptosis (44).

In order to further confirm these observations, indirect immunofluorescence staining was performed by using an anti-active caspase 3 antibody that specifically recognizes the newly exposed C terminus of the 17-kDa fragment of caspase 3 but not the inactive precursor form. As shown in Fig. 2C, the activated form of caspase 3 was clearly observed in HCV-infected cells but not in the mock-infected control at 6 days postinfection. The activation of caspase 3 was observed also at 4 days postinfection (data not shown). We found that caspase 3 activation was detectable in 12% and 21% of HCV antigen-positive cells at 4 and 6 days postinfection, respectively, whereas it was detectable only minimally in mock-infected cells at the same time points (Fig. 2D). These results strongly suggest that HCV-induced cell death is caused by caspase 3-dependent apoptosis. We also observed nuclear translocation of active caspase 3 in HCV-infected cells (Fig. 2E). This result is consistent with previous reports (28, 70) that activated caspase 3 is located not only in the cytoplasm but also in the nuclei of apoptotic cells. Concomitantly, nuclear condensation and shrinkage were clearly observed in the caspase 3-activated cells. As the activation and nuclear translocation of caspase 3 occur before the appearance of the nuclear change, not all caspase 3-activated cells exhibited the typical nuclear changes. Taken together, these results indicate that HCV-induced apoptosis is associated with activation and nuclear translocation of caspase 3.

HCV infection induces the activation of the proapoptotic protein Bax. The proteins of the Bcl-2 family are known to directly regulate mitochondrial membrane permeability and induction of apoptosis (63). Therefore, we examined the expression levels of proapoptotic proteins, such as Bax and Bak, and antiapoptotic protein Bcl-2 in HCV-infected Huh7.5 cells and the mock-infected control. The result showed that expression levels of Bak or Bcl-2 did not differ significantly between HCV-infected cells and the control. Interestingly, however, Bax accumulated on the mitochondria in HCV-infected cells to a larger extent than in the mock-infected control (Fig. 3A), with the average amount of mitochondrion-associated Bax in HCV-infected cells being 2.7 times larger than that in the control cells at 6 days postinfection (Fig. 3B).

In response to apoptotic stimuli, Bax undergoes a conformational change to expose its N and C termini, which facilitates translocation of the protein to the mitochondrial outer membrane (32). Thus, the conformational change of Bax represents a key step for its activation and subsequent apoptosis. We therefore investigated the possible conformational change of Bax in HCV-infected cells by using a conformation-specific NT antibody that specifically recognizes the Bax protein with an exposed N terminus. As shown in Fig. 3C, Bax staining with the conformation-specific NT antibody was readily detectable in HCV-infected cells at 6 days postinfection whereas there was no detectable staining with the same antibody in the mock-infected control. Moreover, the activated Bax was shown to be colocalized with MitoTracker, a marker for mitochondria, in HCV-infected cells. The conformational change of Bax was observed in 10% and 15% of HCV-infected cells at 4 and 6 days postinfection, respectively (Fig. 3D). This result was consistent with what was observed for caspase 3 activation in HCV-infected cells (Fig. 2D). Taken together, these results suggest that HCV infection triggers conformational change and mitochondrial accumulation of Bax, which lead to the activation of the mitochondrial apoptotic pathway.

HCV infection induces the disruption of the mitochondrial transmembrane potential, release of cytochrome *c* from mitochondria, and activation of caspase 9. The accumulation of Bax on the mitochondria is known to decrease the mitochondrial transmembrane potential and increase its permeability, which result in the release of cytochrome *c* and other key molecules from the mitochondria to the cytoplasm to activate caspase 9. Therefore, we examined the possible effect of HCV infection on mitochondrial transmembrane potential in Huh7.5 cells. Disruption of the mitochondrial transmembrane potential was indicated by decreased Rho123 retention and, hence, decreased fluorescence. As shown in Fig. 4, HCV-infected cells showed ~50% and ~70% reductions in Rho123 fluorescence intensity compared with the mock-infected control at 4 and 6 days postinfection, respectively.

Recent studies have indicated that loss of mitochondrial membrane potential leads to mitochondrial swelling, which is often associated with cell injury (27, 50). Also, we and other investigators have reported that HCV NS4A (43), core (53), and p7 (22) target mitochondria. We therefore analyzed the effect of HCV infection on mitochondrial morphology. Confocal fluorescence microscopic analysis using MitoTracker revealed that mitochondria began to undergo morphological changes at 4 days postinfection and that approximately 40% of HCV-infected cells exhibited mitochondrial swelling and/or aggregation compared with the mock-infected control at 6 days postinfection (Fig. 5A and B). It should also be noted that mitochondrial swelling and/or aggregation was seen in a region different from the "membranous web," where the HCV replication complexes accumulate to show stronger expression of